CLIN 0002AE Final Technical Report

for Contract No.: DAAG55-97-C-0033

"Advanced Tunable Optical Filter for Fiber Optic Communication Network"

Dr. I. C. Chang
Aurora Associates
3350 Scott Blvd., Bldg. 20
Santa Clara, CA 95054-3106

May, 2000

20000628 055

REPORT DOCUMENTATION PAGE

Form Approved
OMB NO. 0704-0188

Public Reporting burden for this collection of information is estimated to average 1 hour per response, including the time for reviewing instructions, searching existing data sources, gathering and maintaining the data needed, and completing and reviewing the collection of information. Send comment regarding this burden estimates or any other aspect of this collection of information, including suggestions for reducing this burden, to Washington Headquarters Services, Directorate for information Operations and Reports, 1215 Jefferson Davis Highway, Suite 1204, Arlington, VA 22202-4302, and to the Office of Management and Budget, Paperwork Reduction Project (0704-0188,) Washington, DC 20503.

1. AGENCY USE ONLY (Leave Blank)	2. REPORT DATE May 00	3. REPORT TYPE AND DATES COVERED Final Report 01 Apr 97 - 30 Sep 99

4. TITLE AND SUBTITLE

Advanced Tunable Optical Filter for Fiber Optic Communication Network

5. FUNDING NUMBERS

DAAG55-97-c-0033

6. AUTHOR(S)

I.C. Chang

7. PERFORMING ORGANIZATION NAME(S) AND ADDRESS(ES)

Aurora Associates
3350 Scott Blvd., Bldg 20
Santa Clara, CA 95054

8. PERFORMING ORGANIZATION REPORT NUMBER

9. SPONSORING / MONITORING AGENCY NAME(S) AND ADDRESS(ES)

U. S. Army Research Office
P.O. Box 12211
Research Triangle Park, NC 27709-2211

10. SPONSORING / MONITORING AGENCY REPORT NUMBER

ARO 36692.1-EL-SB2

11. SUPPLEMENTARY NOTES

The views, opinions and/or findings contained in this report are those of the author(s) and should not be construed as an official Department of the Army position, policy or decision, unless so designated by other documentation.

12 a. DISTRIBUTION / AVAILABILITY STATEMENT

Approved for public release; distribution unlimited.

12 b. DISTRIBUTION CODE

13. ABSTRACT (Maximum 200 words)

This report covers Phase II work for the development of dynamically reconfigurable WDM components based on the use of collinear beam acousto-optic tunable filters (AOTF). These include optical add and drop multiplexers (OADM), optical cross-connects (OXC), and dynamic fiber amplifier equalizers (DFAE). The project included three tasks: (A) AOTF performance improvement: new designs and fabrication techniques were investigated. A demonstration model 100GHz channel spacing AOTF was constructed that achieved 0.5nm FWHM, <-25dB sidelobes, 3dB optical insertion loss, <0.1 polarization-dependent loss, and <1psec polarization mode dispersion. (B) Reconfigurable OADM and OXC implementation: various space dilation architectures were examined. Using a 2x2 AOTF, crosstalk reduction was experimentally demonstrated below -25dB. (C) DFAE development: an AO-based system consisting of a multi-wave attenuator, a WDM monitor and a multi-channel electronic controller was constructed. Multi-wavelength operation was demonstrated using a novel modulation decoding scheme. Results show that the use of AO-based dynamic WDM components is the most practical, low-cost approach compared to present "divide and conquer" approaches. As fiber amplifier bandwidth increases further, WDM network channel capacity could be greatly increased by exploiting the AOTF's extremely wide tuning range.

14. SUBJECT TERMS			15. NUMBER OF PAGES 16. PRICE CODE
17. SECURITY CLASSIFICATION OR REPORT UNCLASSIFIED	18. SECURITY CLASSIFICATION ON THIS PAGE UNCLASSIFIED	19. SECURITY CLASSIFICATION OF ABSTRACT UNCLASSIFIED	20. LIMITATION OF ABSTRACT UL

REPORT DOCUMENTATION PAGE (SF298)
(Continuation Sheet)

(1) List of manuscripts:
a. I.C. Chang, "Progress in AOTF Technology," First ARL Workshop on AOTF Technology, Sept. 1996, College Park, MD.
b. I.C. Chang, "Recent Progress of Acousto-Optic Tunable Filters," Invited talk at the 1996 IEEE Ultrasonics Symposium, Nov. 1996, San Antonio, Tx.
c. I.C. Chang, "Acousto-Optic Tunable Filters in Wavelength Division Multiplexing (WDM) Networks," 1997 Conference on Laser and Electro-Optics (CLEO), May 1997, Baltimore, MD.
d. I.C. Chang et al, "Bandpass Response of Collinear Beam Acousto-Optic Tunable Filters," Proc. of IEEE Ultrasonics Symposium, Oct. 1997.
e. I.C. Chang, "Acousto-Optic Wavelength Routing Switch," The Eighth DARPA Symposium on Photonic Systems for Antenna Applications (PSAA-8), Jan. 1998, Monterey, CA.
f. I.C. Chang, "Aacousto-Optic Switch for DWDM Network," SPIE's Asia Pacific Symposium on Optical Fiber Communication, July 1998, Taiwan.
g. I.C. Chang and Jack Xu, "Near Infrared Wide Angle Acousto-Optic Deflector," 1999 Conference on Laser and Electro-Optics (CLEO), May 1999, Baltimore, MD.
h. I.C. Chang and Jack Xu, "Near Infrared Wide Angle Acousto-Optic Deflector," The Ninth DARPA Symposium on Photonic Systems for Antenna Applications (PSAA-9), Feb. 1999, Monterey, CA.

(2) Scientific Personnel:
I.C. Chang and Jack Xu, no honors/awards/degrees during this time.

(3) Report of Inventions
a. Improved Performance Acousto-Optic Tunable Filter and Multi-Wave Multiplexer
b. Multi-Channel Acousto-Optic Multi-Wave Multiplexer and Cross-Connect with Suppressed Coherent Crosstalk
c. Phased Array Acousto-Optic Tunable Filter (Patent Pending)

(4) Summary of the Most Important Results
The most significant theoretical and experimental findings of this program are listed below.
* The use of off-axis tilted acoustic waves for reducing the sidelobes of the AOTF.
* The discovery of new AOTF designs for reducing the temperature and crystal orientation sensitivity for the passband wavelength.
* Development of new architectures for polarization independent (PI) AOTFs.
* Development of efficient dilation architectures for reducing crosstalk due to sidelobes and extinction ratio.
* Proposed and demonstrated the use of a multiple acoustic wave to suppress coherent crosstalk.
* Development of simple architecture and monitoring techniques for the operation of the DFAE.
* Built the DFAE system and demonstrated the feasibility of multi-wave operation.
* Built, tested and developed the prototype for near-term commercialization of a) low-cost WDM monitor, b) single-wavelength dynamic OADM, and c) single AOTF automatic gain equalization.

(5) Technology Transfer
Experimental verification (put into practice) some patents as listed below.
a. US 5,576,880, Wide Angle Acousto-Optic Modulator
b. US 5,904,304, Intrinsically Polarization-Independent Acousto-Optic Tunable Filter
c. US 6,016,216, Polarization Independent Acousto-Optic Tunable Filter

TABLE OF CONTENTS

1.0 Introduction

1.1 Identification and Significance of the Problem

The final report covers work performed in Phase II of the SBIR contract entitled "Advanced Tunable Optical Filter for Fiber Optic Communication Network." The program objective is to develop an advanced tunable narrowband optical filter for use in wideband fiberoptic communication networks.

The deployment of passive dense (D) WDM into point-to-point long-haul communication network has realized the objective of providing low-cost wideband transport in the core network. In this first generation of optical transport network (OTN) utilizing DWDM, nearly all of the networking functionality remains in the SONET/SDH based time domain multiplexing (TDM) system. The emerging WDM products are now entering the second generation of OTN, which is aimed at extending the wideband service from the core to local area and metropolitan applications as well as adding the functionality of switching, routing, supervision and survivability in the optical domain. To achieve these goals will require development of the dynamic reconfigurable WDM components that includes dynamic optical add and drop multiplexer (OADM), optical cross-connects (OXC) multi-wave spectral monitor, dynamic fiber amplifier equalizer (DFAE), and protection bypass switches.

The present approach for constructing such dynamically re-configurable WDM cross-connect is to use passive fixed wavelength Mux/Demux and wavelength independent space division multiplexing (SDM) switches. At the input ports, the multi-wave signals are broken by a passive WDM Demux into separate channels of single wavelength. Each of these single wavelength signals are switched by an array of SDM switches and are then recombined by the output WDM Mux. Obviously, such a "divide and conquer" scheme is locked into the specific wavelength allocations. Moreover, as the number of wavelengths increases, the physical construction of the WDM cross-connect becomes significantly complex. For a 2x2 WDM cross-connect with N number of wavelengths, a total of 4N interconnecting fibers and N 2x2 non-blocking SDM switches are needed. Furthermore, the only presently available SDM switches are mechanically tuned and suffer from the inherent limitation of slow switching speed (typically longer than 10 milliseconds). Since a major important goal in the second phase of the OTN is to deploy optical layer protection and restoration structures, the low-speed mechanical switches can not meet the overall system switching time requirement

An alternative approach to realize the reconfigurable WDM cross-connect is to use a wavelength selective switch known as the Acousto-Optic Tunable Filter (AOTF). The AOTF has the unique capability of being able to simultaneously and independently add or drop multi-wavelength signals. As such, it can serve as a true WDM cross-connect for routing multi-wavelength optical signals along a prescribed connection path determined by the signal's wavelength.

Because of the unique wavelength selective capability, an AOTF using an integrated configuration was chosen by the Optical Network Technology Consortium (ONTC) [1] as the core device in the all-optical network (AON) proposed for the national information infrastructure (NII). More recently, the integrated (I) AOTF-based WDM cross-connect was deployed by the National Transparent Optical Network Consortium (NTONC) in a testbed demonstration at the Berkeley-Livermore-San Ramon site [2].

The IAOTF [3] is the integrated or waveguide version of the bulk wave collinear AOTF [4] and thus suffers high coherent crosstalk resulting from the imperfect polarization splitting of the collinear geometry. The tight fabrication tolerance required in the construction of the polarization independent (PI) AOTF in the integrated optic implementation also results in high polarization dependent loss (PDL), large polarization mode dispersion (PMD), and excessive manufacturing cost. In bulk versions, the matured technology of noncollinear AOTF has been deployed in a variety of optical sensor and spectroscopy applications [5]. However, due to the acoustic beam walkoff, the bulkwave AOTFs is unsuitable for WDM because of its drawbacks of poorer resolution and higher drive power.

Recently Aurora Associates invented a new type of bulkwave PI AOTF that overcomes these deficiencies. The collinear beam (CB) AOTF [6] combines the attractive features of IAOTF and the bulkwave noncollinear AOTFs [7]. During the Phase I effort, a high-performance polarization independent (PI) CBAOTF feasibility model was designed, built and demonstrated. The measured performances at 1550nm included; bandwidth: 1nm, sidelobe: 27dB at 3.2nm spacing, insertion loss: 3dB, drive power: 100mW, PDL: 0.1dB, and PMD: 1psec. While such performances satisfy the requirements for tunable filter applications at about 400GHz spacing, the CBAOTF is yet inadequate for use as the dynamic WDM switching components due to the unacceptable levels at narrower channel spacing. It is the primary objective of the Phase II effort to overcome the critical limitations and extend the useful operation to channel spacing of 100GHz.

This report is organized into the following sections. Section 2 reviews the problem and discusses the proposed approaches. Section 3 describes the PIAOTF with enhanced performance. Section 4 presents the results of the AO-based dynamic OADM and OXC. Section 5 discusses the development of the AO-based DFAE. Finally, Section 6 presents the conclusions of the Phase II work.

1.2 Phase II Technical Objective

The overall technical objective of the Phase II effort is to develop low cost, high performance AOTFs for use as dynamic WDM components. The initial objective was to meet the design goals of 200 to 400GHz channel spacing. However, since the completion of the Phase I work, progress on the passive WDM technology has pushed the "standard" channel spacing to 0.8nm. To be compatible with the backbone WDM network, the AO-based dynamic WDM components must be able to achieve the same wavelength spacing requirements. The modified objectives for the Phase II tasks are:

Task I Multi-Wave Tunable Filter (MWTF)

The objective is to develop a 100GHz channel spacing PIAOTF with the performance goals listed in Table 1-1.

Table 1-1 Modified Performance Goals of AOTF for WDM

Wavelength Range:	1300-1600nm
Center Wavelength:	1550nm
FWHM:	0.4nm
Wavelength Spacing:	0.8nm
Sidelobe Level:	25dB
Extinction Ratio:	25dB
Insertion Loss:	3dB
PDL:	0.1dB
PMD:	<1psec
Drive Power:	150mW/signal

1. **Performance Improvement** - Develop performance improvement techniques for suppressing sidelobes, temperature sensitivity and reducing manufacturing difficulties.
2. **Prototype Development** - Design, build, test and evaluate the prototype MWTF.

Task II Multi-Wave Cross-Connect (MWXC)

The objective is to develop the AO based MWXC for use as a dynamic OADM & OXC.

1. **Critical Crosstalk Issues** - Develop architecture and designs for reducing crosstalk.
2. **Dynamic OADM/OXC** - Develop a prototype OADM and extend to multi-wave OXC

Task III Dynamic Fiber Amplifier Equalizer (DFAE)

The objective is to develop an AO-based feedback controlled multi-wave attenuator for controlling the power levels of multi-wave optical signals in a WDM network.

1. **Multi-wave optical spectral analyzer (MOSA)** - Develop a MOSA for sampling, analyzing and monitoring the amplitude of multi-wavelength signals.
2. **Multi-Channel Electronic Controller (MCEC)** - Design, build and test a multi-frequency programmable RF source for controlling the amplitudes of multi-wavelength signals.
3. **DFAE Integration** - To integrate the MWTF, MCEC, and MOSA into a DFAE system for dynamic power equalization of multi-wave signals in WDM network.

2.0 Problem and Proposed Approach

2.1 Requirements of Tunable Filter to WDM Network

The ever-growing demand for more bandwidth in fiberoptic communication has stimulated the rapid development of WDM technology. Due to the intrinsic dispersion of optical fibers, the usable bandwidth for single wavelength transport is limited to about 2.5Gbits, and the traditional time-domain multiplexing (TDM) techniques are no longer economically viable. More importantly, in a TDM based network, the increasingly large bandwidth requirement severely stresses the bit rate of the front-end electronics, which creates the so-called TDM bottleneck.

In this first generation of optical transport network (OTN), the deployment of the WDM has been restricted to point-to-point and the broadcast optical star telecommunication link. Figure 1 shows the present backbone of the WDM network to the long haul point-to-point telecommunications link. The key components (other than the passive DWDMs) to support such

a WDM network include the laser transmitters (DFB laser and external modulators), in-line fiber amplifiers and tunable receivers

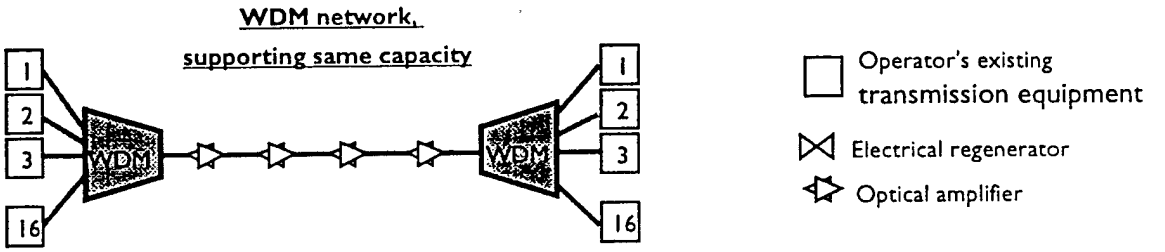

Figure 1 Present Backbone of WDM Network to Point-to-Point Telecommunication Link

Figure 2 shows the schematic of a multi-wavelength Broadcast Optical Star Network. An essential component in both of these WDM architectures is a tunable narrowband optical filter used for selecting and adjusting the power levels of the optical signals based on wavelength. In the broadcast star network shown in Figure 2, the tunable filter is used to tune the receiver or laser transmitter or possibly both.

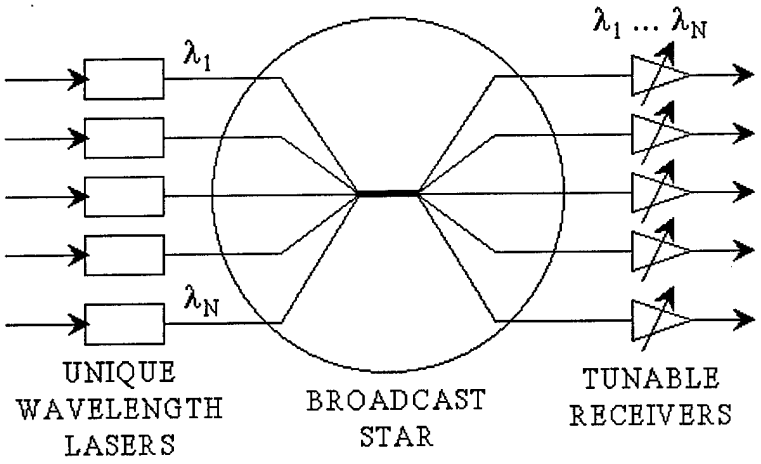

Figure 2 Multi-Wavelength Broadcast Optical Star Network

Other applications of the multi-wave tunable filter includes wavelength lockers and dynamic fiber amplifier gain equalizers. Of particular importance in WDM systems is the stability of the source wavelength in each channel. Any drift in the laser wavelength can cause signal cross talk between channels and other undesirable effects. Because the PI-AOTF can be scanned to locate the peak wavelength of all WDM channels in single scan, only one device is required to provide feedback signals for locking each source laser controller.

Another important application of the tunable filter for WDM communication network is to equalize the fiber amplifier gain profile [9]. Presently, in-line Erbium-doped fiber amplifiers (EDFAs) are used as gain blocks in multi-wavelength fiber optic networks. These amplifiers have a gain profile that varies about 7dB in the 1.55μm range. In order to flatten the response, fixed optical filters are used. However, in reality, the accumulated insertion loss for a given wavelength signal as it propagates through the various nodes of the network is dynamically changing due to continuously changing path configuration. What is needed is a multi-passband

filter that can be continuously reprogrammed to the corrected spectral profile in order to achieve channel equalization of the optical signals. In this case, the tunable filter must be able to operate at multi-wavelengths with independent amplitude control of the optical signals.

The emerging WDM products are now entering the second generation of OTN, which is aimed at extending the wideband service from the core to local area and metropolitan applications as well as adding the functionality of switching, routing, supervision and survivability in the optical domain. To achieve these goals will require development of the dynamic reconfigurable WDM components that includes dynamic optical add and drop multiplexer (OADM), optical cross-connects (OXC) multi-wave spectral monitor, dynamic fiber amplifier equalizer (DFAE), and protection bypass switches.

In the most advanced architecture of wavelength routing networks shown in Fig. 3, the use of such dynamic reconfigurable WDM components provide an efficient approach for routing multi-wavelength optical signals along a prescribed connection path determined by the signal's wavelength. Thus, by using the wavelength as a routing tool, the wavelength routing network can realize a multiplicity of signal interconnection patterns with fixed optical system hardware.

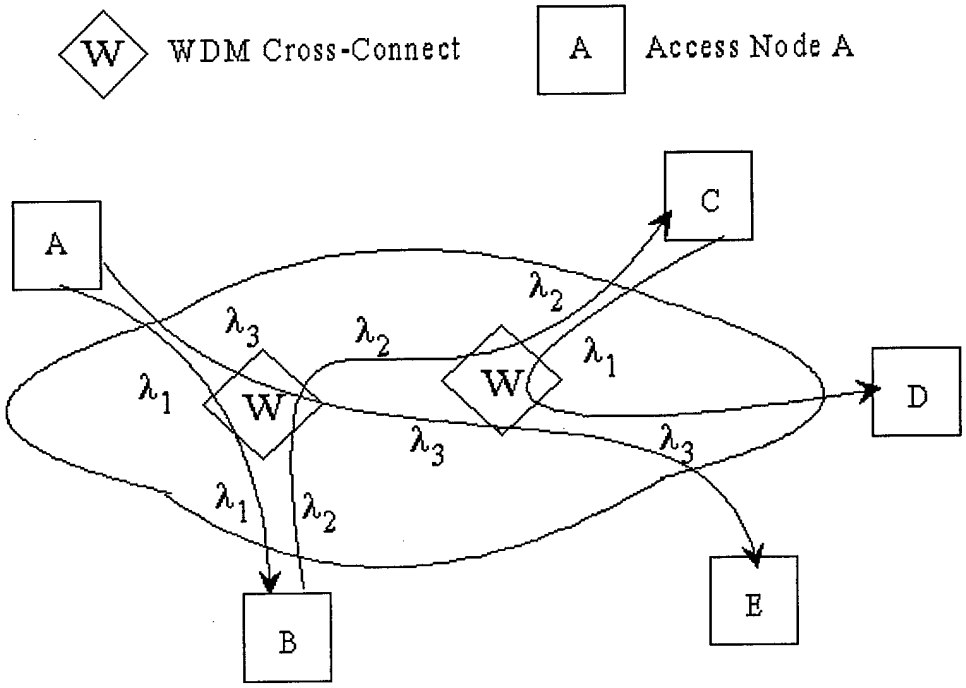

Figure 3 Wavelength Routing Network

The present WDM network is based on the use of fixed wavelength passive Mux/Demux. Using this scheme, the optical node of the network must be associated with a fixed wavelength. To realize wavelength routing, it is necessary to implement dynamically reconfigurable (R) OADM or OXC. The present approach for such reconfigurable WDM components is to use passive Demux to decompose the input multi-wavelength signals into N multiple channels, providing the cross-connects using N space-division-multiplexing (SDM) switches and recombine the outgoing signals using another DWDM as Mux. For example, Fig. 4 shows a ROADM that allows the adding and dropping of a selected set of wavelength channels from a DWDM multi-channel stream. The use of the SDM switches and attenuator in each separate channel are used to perform the channel switching and signal amplitude control. The system

hardware for implementing such "divide and conquer" scheme becomes increasingly complex and costly as the number of wavelengths N becomes large. For instance, to construct a simple 32-channel ROADM, a total of two 32-channel DWDMs, thirty-two 2x2 switches, thirty-two attenuators and 160 interconnecting fibers are needed.

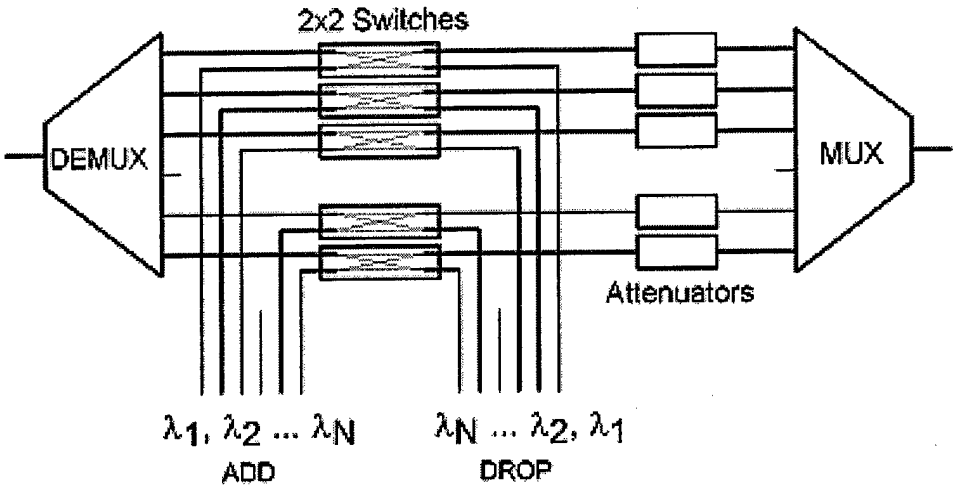

Figure 4 ROADM

An alternative approach is to realize the desired function in the wavelength routing network is to use the tunable filter as a wavelength selective cross-connect (WSXC). For this application, the functional requirement for the tunable filter in the wavelength routing network is more demanding than that for tunable receiver. As a WSXC, the tunable filter must demonstrate the capability to simultaneously and independently route multiple wavelength signals. Compared to the space domain switches, the use of tunable filters or WSXC is more efficient in reconfigurable WDM networks for increasing the number of wavelengths. The tunable filter approach is particularly economical for the optical interconnection with a small number of input and output ports.

In addition to the multi-wavelength capability, the tunable filter must meet the following performance requirements:

a. Large tuning range - The minimum tuning range of the tunable filter is determined by the bandwidth of Erbium-doped fiber amplifier (EDFA). Due to the recent extension of EDFA into the S and L bands, the required spectral range for future WDM systems is expected to approach the low attenuation band of silica fiber at 1550 nm, i.e. about 200nm.
b. Small channel spacing - To maximize the number of wavelength channels within the tuning range, a small channel spacing less than 0.8nm is required.
c. Narrow bandwidth - To be compatible with the present ITU standard, a narrow passband is required in order to satisfy the mall channel spacing requirement. For a channel spacing of 0.8nm, the full width half maximum (FWHM) is typically 0.4nm.
d. Low sidelobe - The primary source of crosstalk induced in the filter is the high level of sidelobes. For acceptably low crosstalk, the sidelobe (or skirt ratio) at the channel boundary must be sufficiently low (~25dB).

e. Low optical insertion loss - An obvious requirement is low optical insertion loss from the single mode fiber (SMF) through the tunable filter and back to the SMF (<3dB).

f. Fast switching speed - For circuit switching, moderate reconfiguration time (< 1 millisec) is adequate.

g. Low drive power - Since the drive power for simultaneous multi-wavelength filtering is proportional to the number of wavelengths, a low drive power per channel is required (<100mW).

h. Polarization independent - To be compatible with fiber optic networks, operation of the tunable filter must be independent of the polarization of the input optical beam.

2.2 Acousto-Optic Tunable Filter

2.2.1 Integrated Acousto-Optic Tunable Filters

A number of tunable filter technologies have been studied as potential candidate approaches for making dynamic WDM components. These include the mechanically tuned Fabry-Perot filter (FPF), the liquid crystal (LC) tuned filter, the electro-optical tuned filter (EOTF) and the acousto-optic tunable filter (AOTF). Among them, the AOTF is the only type that has the unique multi-wavelength capability.

Figure 5 shows the schematic of a polarization-independent integrated AOTF [10]. The input beam is divided by the polarizing beam splitter (PBS) in to two components, TE and TM modes, which pass through the interaction region in two separate paths. Both components of the input optical beam at the selected wavelengths are diffracted into the orthogonal polarization (TE «TM). The switched light at the selected wavelengths in the two optical paths are combined by the polarizing beam combiner and appear as the filtered light in the lower channel. Unswitched components recombine by the polarizing beam combiner and appear as the unfiltered light in the upper channel.

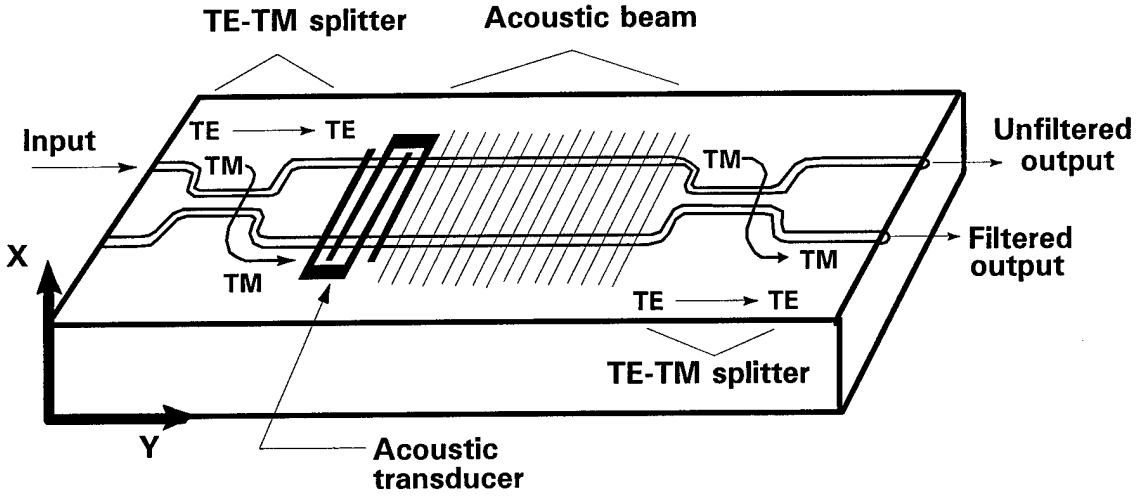

Figure 5 Schematic of the Polarization-Independent Integrated AOTF

Significant progress on IAOTF technology has been made in recent years. Table 2-1 shows the specifications of a state-of-the-art IAOTF with the best overall performance [7].

Table 2-1 Performance of CBAOTF for WDM Cross-Connect

Parameters	**IAOTF**
Material	x-cut, y-prop. $LiNbO_3$
Interaction geometry	double stage
Center wavelength	1550nm
Tuning range	1526 to 1602nm (76nm)
FWHM	1.4nm
Drive power (per channel)	80mW
Sidelobe	-14dB
Optical loss (fiber pigtail)	(fiber to fiber) 4.8dB
Polarization dependent loss (PDL)	0.2dB
Polarization mode dispersion (PMD)	not measured

The above table shows that the most critical performance limitations of the IAOTF technology are high sidelobes and polarization dependent degradation and construction complexities. These basic deficiencies of the IAOTF are discussed below.

High Crosstalk

There are three kinds of crosstalk: (1) The first source of crosstalk is due to incomplete polarization conversion of the AOTF and the light leakage of the polarizing beam splitters (PBS) that must be used in a collinear IAOTF in order to separate the filtered output beam from the input beam. (2) The second kind of crosstalk is due to the high sidelobe level resulting from the inhomogeneous birefringence of the $LiNbO_3$ waveguide. (3) A third source of crosstalk is coherent intermodulation, which originates from the mixing of two collinearly propagating optical waves inside one wavelength channel [3].

Polarization Dependent Degradation

The IAOTF is inherently polarization dependent since its operation is based on anisotropic diffraction in a birefringent crystal. The device can be constructed to be polarization independent by using the polarization diversity configuration. To minimize the polarization dependent loss (PDL) and polarization mode dispersion (PMD), the two optical arms for TE and TM modes must be accurately balanced with equal insertion loss and group delay time. This requirement cannot be met in practice for the IAOTF since there is no mechanism for fine tuning the balance in an integrated structure once fabrication is completed.

Fabrication Complexity

The polarizing beam splitter (PBS) is a critical part of the IAOTF. However, until now, the development of a high rejection waveguide-type PBS that can be integrated on the same substrate with the IAOTF has not been successful. Consequently, the present approach uses a hybrid structure that connects external bulk PBS to the IAOTF by means of polarization-preserving fibers (PPFs). Construction of such hybrid device structure presents severe fabrication problems.

High Insertion Loss

The coupling between the waveguide, free space and the single mode fiber (SMF) on the hybrid structure yields high insertion loss, typically about 6 dB. Furthermore, in order to reduce

the crosstalk, the use of space dilated architecture requires multiple in and out couplings from the $LiNbO_3$ waveguide to free-space. The optical insertion loss of a dilated IAOTF exceeds 11dB.

2.2.2 Bulkwave Acousto-Optic Tunable Filter

Fig.6 shows the schematic of a bulkwave AOTF configuration that utilizes noncollinear interaction of acoustic and optical waves. [6]. The bulkwave AOTF offers three major advantages: (a) a broader class of more efficient AO materials is available. For instance, the AO figure of merit of TeO_2 is about 50 to 100 times that of $LiNbO_3$. (b) The bulkwave geometry allows simpler and more flexible fabrication and can be easily integrated with other optical components in a free-space interconnection configuration. (c) The three-dimensional spatial structure of the bulkwave device allows the possibility of scaling to a large number of ports.

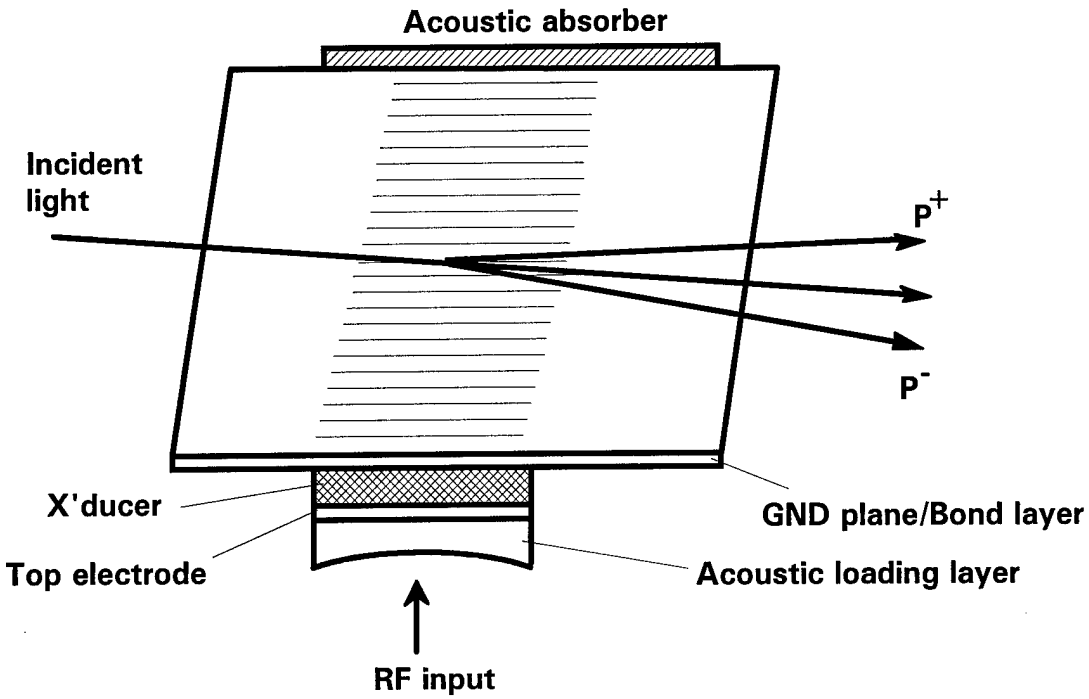

Figure 6 Noncollinear Bulkwave Acousto-Optic Tunable Filter

For WDM applications, the noncollinear AOTF has a major drawback. The large acoustic beam walkoff limits the maximum interaction length obtainable and thus results in low resolution and high drive power. To solve this critical issue a new type of noncollinear AOTF, the collinear beam (CB) type, was proposed and demonstrated [6]. By choosing the group velocities of the optical and acoustic waves to be collinear, an extended interaction length was realized in a TeO_2 AOTF with drastically lower drive power and narrow bandwidth. Compare for example, the performance of a CBAOTF with the conventional type TeO_2 AOTF. The specified parameters of the AOTF at 1.55μm are: L=33mm, H=2mm, D=2mm, optical angle θ_o=45°, and 3dB transducer loss. The required RF power per signal values at 100% efficiency are 18 and 300mW, respectively for the CB and conventional type of AOTFs. The drastically lower RF power is the most significant advantage of the CBAOTF for WDM applications that requires switching of a large number of optical signals. Actual drive power will be higher when the additional loss due to acoustic attenuation, diffraction and acoustic beam walkoff are taken into account. With proper crystal orientation, the maximum drive power per wavelength is estimated to be about 50mW.which is about the same level as that of the LAOTF. Thus, the bulkwave CBAOTF can realize the lower power advantage of the IAOTF and meanwhile has the benefits of the bulkwave device that include design flexibility, choice of materials and lower manufacturing cost.

2.3 Collinear Beam AOTF

2.3.1 Characteristics of CBAOTF

Figure 7 shows the schematic of a TeO_2 CBAOTF using an in-line Internal Mode Conversion (IMC) configuration. The in-line configuration simplifies the optical alignment and reduces the optical insertion loss for coupling to the SMF. Since the input and output faces of

the CBAOTF are parallel and normal to the o-order light beam, the in-line structure also minimizes the angular deviation due to dispersion.

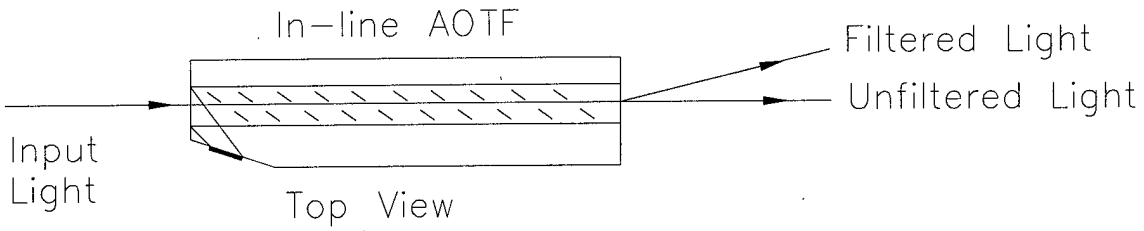

Figure 7 In-Line CBAOTF using Internal Mode Conversion Arrangement

The CBAOTF is intrinsically polarization dependent. Similar to the IAOTF, a polarization independent (PI) version can be constructed using the polarization diversity configuration (PDC), i.e. the scheme of dividing into two polarizations, selecting the optical beams of given wavelengths and recombining the selected beams of two polarizations. Unlike the IAOTF, however, the basic characteristics (i.e. wavelength, frequency and angular relation) are unsymmetrical for ordinary (o) and extraordinary (e) rays. To realize a PI version, the basic characteristics of the CBAOTF were examined for light beams of both ordinary and extra-ordinary polarizations. The results are summarized below.

Tuning Relation

The f-λ relation of the CBAOTF was obtained by requiring the phase matching condition and collinearity of acoustic and optical beams. At 1.55μm, the acoustic frequencies for the e- and o-waves, f_o and f_e are approximately linear over the angular range of 20 to 60 degrees and vary between 15 and 45MHz with a frequency difference equal to 1.1MHz. This corresponds to a wavelength difference of 45nm.

Bandwidth

The FWHM of a TeO_2 CBAOTF in wavenumber is approximately equal to $7.13/(L\sin^2\theta)cm^{-1}$ or $(1.7/\sin^2\theta_o)nm$ per centimeter of interaction length. A large angle is preferred in order to achieve a narrower FWHM per unit length. However, there are three disadvantages of choosing a large optical angle: (a) the acoustic frequency is higher and consequently there is a higher acoustic attenuation per unit length. (b) $\mathbf{M_2}$ value drops rapidly when θ_o exceeds 30°. (c) At large θ_o values, the acoustic angle $\theta_a \rightarrow 90°$. At close to 90°, the acoustic anisotropy is large, this introduces high diffraction loss and more importantly, the tolerance on the crystal orientation (x-ray) becomes extremely critical. Based on the above considerations, an optical angle of 45° is chosen.

Polarization Independence

Since the basic principle of the AOTF is based on birefringent diffraction in an optical anisotropic medium. The device characteristic depends critically on the polarization state of the incoming light beam. To make it polarization independent, polarization diversity configurations (PDL) are used. The scheme achieves PI by dividing into two beams of orthogonal polarization, o- and e-rays with a polarization beam splitter (PBS) passing through two single polarization AOTFs in two paths then combing the two diffracted o- and e-rays of selected wavelengths with a second PBS. Unlike the IAOTF, however, the AO diffractions for the o- and e-rays are unsymmetrical. To resolve this problem, a novel approach was chosen wherein the polarization

of one beam exiting from the PBS, for instance the o-ray, is converted to the orthogonally polarized o-rays so that two identical single polarization AOTFs are used in the two paths. Since the AOTF operation for fiber optic communication is within a small wavelength range, the required polarization switching can be obtained by using half-wave plates. A number of PDCs are developed. Fig. 8 shows a Type I PDC using two parallel paths [8].

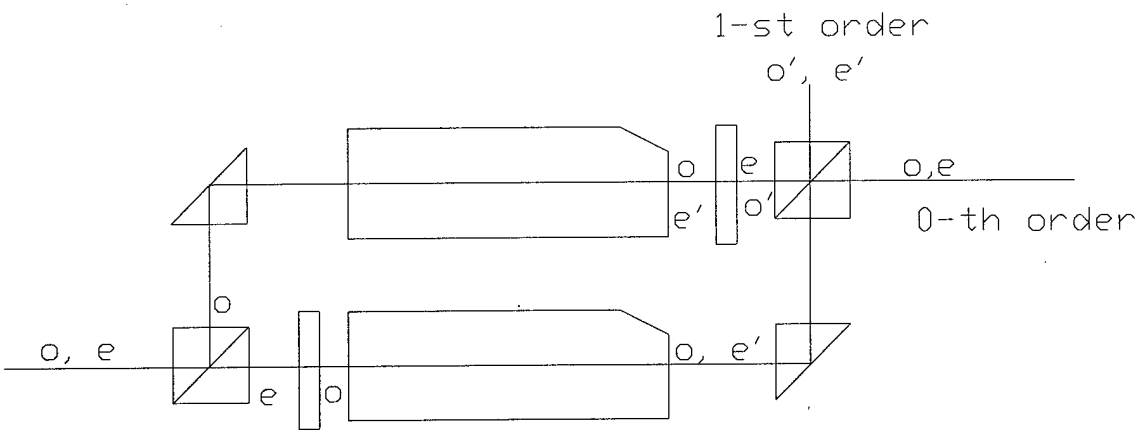

Figure 8 Type I, Parallel PD AOTF Configuration

The operation of a parallel PDC (Type I) is described as follows: the randomly polarized input light is split by the input polarizing beam splitter (PBS) into o- and e-beams. The e-beam is converted into an o^1-beam by passing through a half-wave plate. The two optical beams, o- and o^1-, are allowed two identical CBAOTFs designed for ordinary input. One of the diffracted light beams (e-beam) is converted back to ordinary polarization. The pair of diffracted light beams is then recombined by the output PBS. The configuration also provides other benefits: (a) the frequency shift for both o- and e- are the same (up or down), thus avoiding the problem of coherent crosstalk due to interference; and (b) the o- and e- paths are symmetrical, allowing easy adjustment of the optical path to minimize PMD and PDL.

Another scheme is the serial type (Type II) PDC (shown in Fig.9). In the serial type of AOTF configuration the total optical loss is higher then that for the Type I. However, the diffracted rays for the two polarizations are parallel and thus can be easily combined into a single AOTF. This greatly simplifies the alignment process and is certainly more cost effective. The disadvantage is the overall long lengths of the two AOTF crystals, plus the added complexity of the beam forming optics.

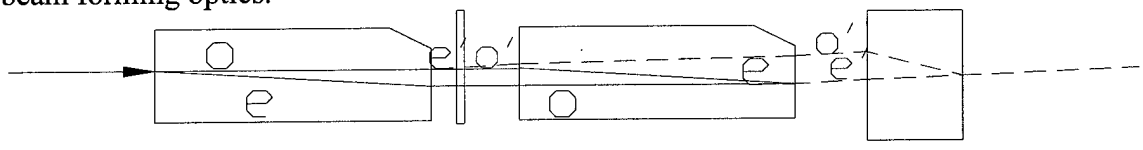

Figure 9 Type II, Serial Type PD AOTF Configuration

2.3.2 Measured Performance of CBAOTF

To verify the theoretical projection, an in-line 45-degree CBAOTF was designed, fabricated and tested [9]. The bandpass response of the CBAOTF was measured by sweeping the acoustic frequency across the diode laser line at 1550nmws A laser diode at 1550nm was

used as the light source in the experiment. The laser beam was ordinarily polarized and coupled into the TeO_2 AOTF and propagated along the long axis of the crystal, i.e., collinear with the acoustic beam. Fig.10 shows the bandpass response of the filter obtained by monitoring the diffracted light intensity as the acoustic frequency was swept through the laser line.

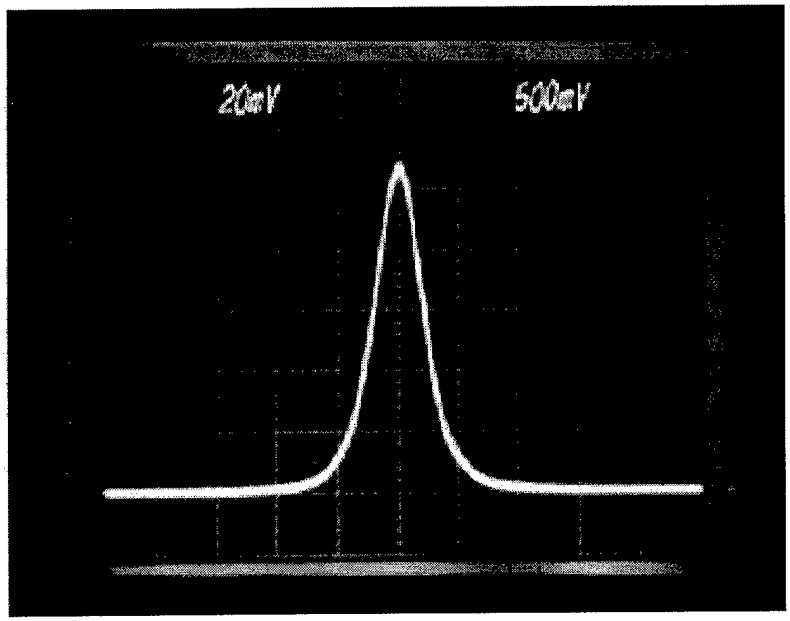

Figure 10 Bandpass of CBAOTF as RF is swept Through a Laser Line at 1.550μm.

The transmission of the diffracted light reaches peak amplitude when the acoustic frequency is about 38.24MHz. The measured acoustic frequency bandwidth of 25KHz corresponds to an optical filter FWHM of (1550)(0.25)/38.24 ~1nm at 1.550nm, or 4.3cm^{-1} if measured in wavenumber. The measured FWHM of the passband was about 1nm

Sidelobe:

As shown in Figure 10, the high sidelobes (~-10dB) of bandpass observed in a conventional AOTF was clearly absent. Closer examination of the sidelobe using detector/amplifiers of increased gain shows that there is no detectable sidelobe down to about -30dB. However, the bandpass response of the CBAOTF decreases slowly at a falloff rate of -6dB per octave wavelength change. The falloff rate is the same as the envelope of the $sinc^2$ response of the conventional AOTF. For fast falloff of the bandpass response, suitable apodization of the acoustic profile is needed.

Efficiency and Drive Power:

The filter efficiency was also measured as a function of drive power. The diffracted light reaches 90 percent when the input RF power is 50mW. Like the conventional AOTF, the peak diffraction efficiency of the CBAOTF also saturates to a peak value of 95% when the drive power is increased to about 55mW. Further increase of drive power results in a decrease of the diffraction efficiency. Figure 11 shows the measured diffraction efficiency of the CBAOTF as a function of drive power.

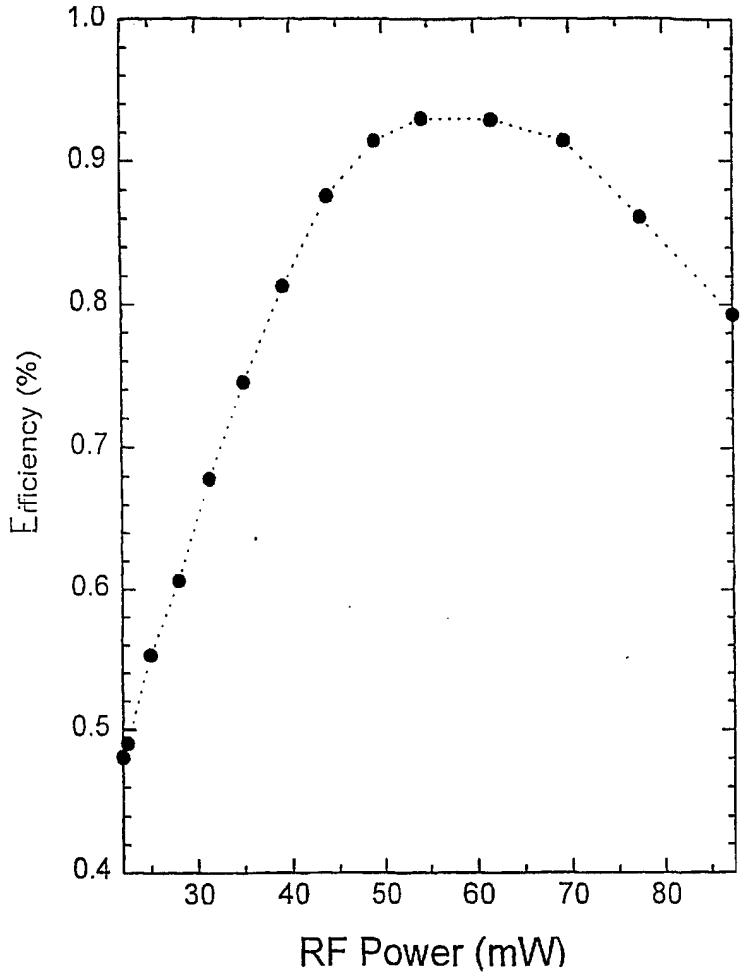

Figure 11 Measured Diffraction Efficiency of the CBAOTF as a Function of Drive Power

Angular Dependence:

In contrast to the conventional AOTF, the filter passband wavelength (or acoustic frequency for a fixed wavelength of the CBAOTF) is linearly proportional to the change of incidence. Because of this angular shift of frequency, the passband becomes broadened for a finite cone of incident light. To avoid this, the input laser beam must be well collimated. In practice, a SMF collimator with a larger input aperture (~1.3mm) is used.

Figure 12 shows the measured results of the angular dependence. The frequency shift is about 1% per degree.

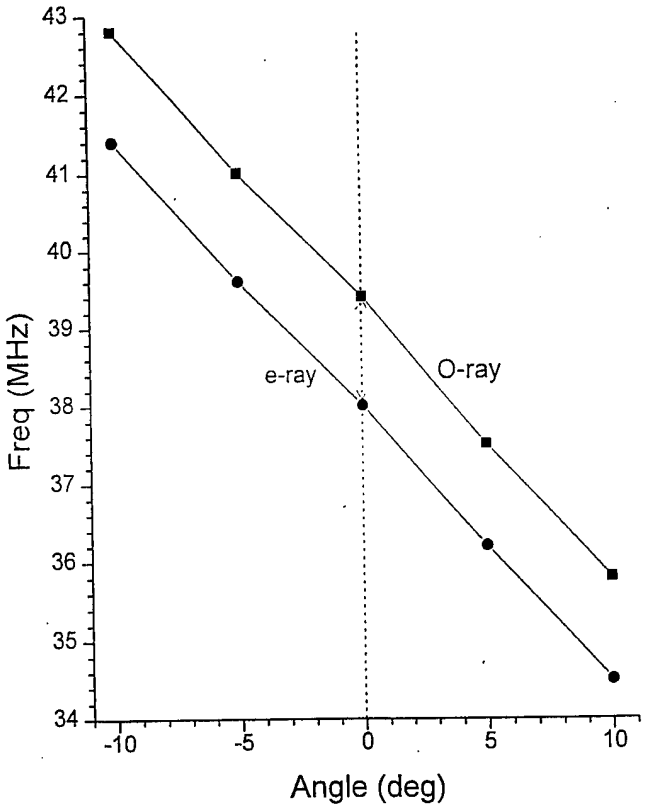

Figure 12 Frequency of CBAOTF vs. Incident Angle for Ordinary and Extraordinary Ray Input

Figure 12 also shows the difference between the incident beams of two polarizations (o- and e-ray). At the same input angle, the frequency shift is nearly a constant (1.08MHz). This corresponds to about 43nm in wavelength difference. Thus, two light beams of different wavelengths and polarizations can be independently selected without introducing in-band spurious signals (ghosts).

3.0 Performance Improvement

3.1 Bandpass Control

The bandpass response of the AOTF for an incident optical plane wave is equal to the longitudinal modulation transfer function of the acoustic field along the optical path. For uniform acoustic field distribution, it reduces to the familiar sinc^2 function, i.e.

$$H(\Delta s)=\text{sinc}^2\Delta sL$$

where $\Delta s=\Delta k/2\pi$ is the spatial frequency mismatch of the AO interaction and L is the optical path. To the first order of the angle deviation $\delta\theta_o$ from the chief ray direction, Δs is approximately given by:

$$\Delta s=b\sin^2\theta_o\delta y+y\Delta n\{\sin 2\theta_o-\sin^2\theta_o\tan(\theta_a-\theta_o)\}\delta\theta_o$$

where θ_o and θ_a are the polar angles of the optical and acoustic waves, respectively, $y=1/\lambda$ is the optical wavenumber, Δn is the birefringence and $b=\delta/\delta y(y\Delta n)$.

The above plane wave solution can be used to determine the filter bandpass for a divergent optical beam by integrating over the divergence angle $\Delta\theta$. Since the CBAOTF is critically phase matched, the filter bandpass can be changed as $\Delta\theta$ increases. Figure 13 shows the calculated CBAOTF bandpass for several choices of cone angle $\Delta\theta$. It is seen as the result of finite optical divergence that the CBAOTF bandpass response becomes broadened but with less distinct sidelobes. However, the rolloff ratio versus the deviation from the peak wavelength is not significantly changed.

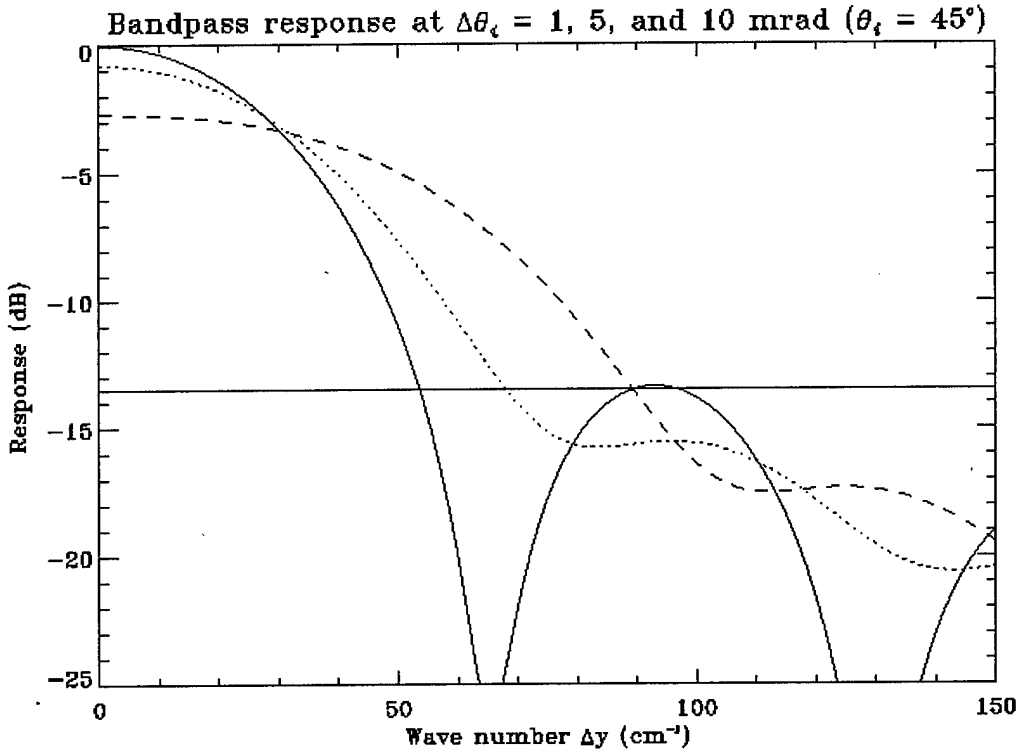

—— = *1mrad,* ------ = *5mrad,* ····· = *10mrad*

Figure 13 Calculated Bandpass of CBAOTF for Divergent Light Beam with Cone Angle $\Delta\theta$

Sidelobe Suppression

One of the most critical issues of the CBAOTF is the high sidelobes of the bandpass characteristics. Theoretically, the fall of the rate in the CBAOTF is the same. To realize a faster rolloff bandpass response, certain forms of apodization of the acoustic field along the optical path are needed. The important questions to be answered are (a) what type of apodization is needed to obtain the sidelobe of -30dB? and (b) how do we implement the desired apodization to the basic collinear beam structures?

By choosing an appropriate window, low sidelobes are obtainable. The window is chosen to that the sidelobe is lower than 30dB, which occurs at minimum wavelength separation for a given filter length. Using a simple model for the apodized AOTF, the bandpass is given by the power spectrum (i.e., Fourier transform square) of the window function. Table 3-1 lists the sidelobe levels of apodized AOTF with different choices of weighting functions.

Table 3-1 Sidelobes vs. Wavelength Spacing (nm) for 1cm Long AOTF (θ_o=45°)

Weighting	Hamming	Triangle
-3dB	1.72	1.65
-20dB	4.05	3.71
-30dB	4.66	4.13
-40dB	5.0	-

The Hamming window yields the lower sidelobes, yet a triangular window is more easily implemented in the CBAOTF by using a walkoff configuration. To achieve a -30dB sidelobe level at 0.8nm, theoretically the minimum length of the CBAOTF would be 5.2cm. In practice, this length would be too long. To shorten this length, it is preferable to change to a 70° design. The overall length of the CBAOTF for 0.8nm spacing would then be about 3cm.

A simple technique of applying amplitude weighting is to arrange an acoustic beam walkoff from the optical beam [10]. For acoustic wave propagation in a highly anisotropic medium such as TeO_2, there will be a larger acoustic beam walkoff away from the <110> plane. Therefore, the acoustic transducer normal is chosen to be tilted from the <110> plane. Such an acoustic beam walkoff will result in an acoustic apodization with a triangular window. Theoretically, the maximum sidelobe is about 26dB below the main peak. Figure 14 shows the acoustic beam walkoff from the <110> plane of the TeO_2 CBAOTF. The simple apodization thus exploits the three-dimensional interaction geometry of the bulkwave AOTF.

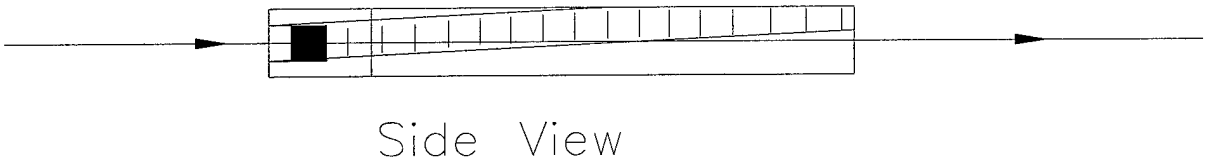

Figure 14 Acoustic Beam Walkoff in TeO_2 CBAOTF

The apodization resulted from the tilted plane structure is approximately equivalent to a trapezoidal window. The filter rolloff characteristic is a function of the parameter β, defined as the length ratio of the top to the bottom of the trapezoid. Figure 15 shows a special trapezoidal window (β=0.16). This is a good approximation to the Hamming window, also shown in Fig. 15. Notice that in the limit, the weighting window reduces to triangular (β=0) and rectangular (β=1).

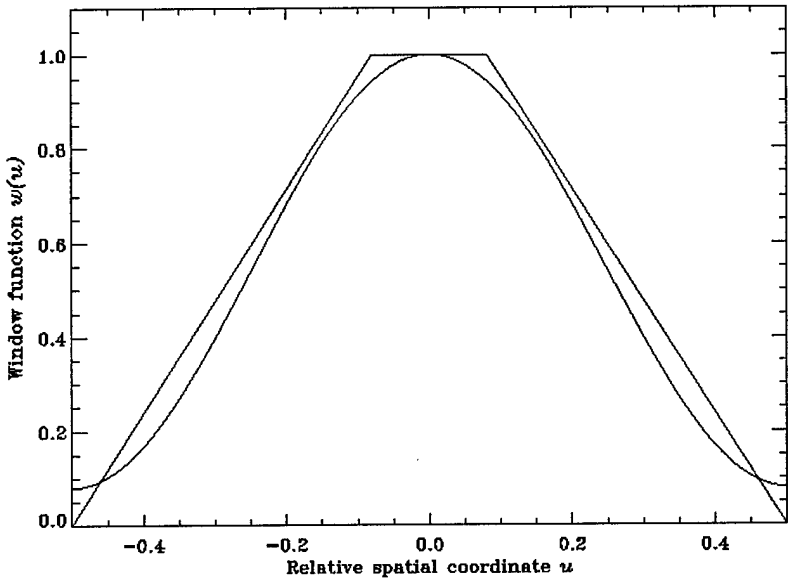

Figure 15 Trapezoidal vs. Hamming Window

The bandpass characteristics of the CBAOTF using trapezoidal windows was calculated in the plane wave approximation. The result for β=0.16 is shown in Figure 16. The filter bandpass for β=0.16±0.02 is seen to be an optimum choice. In this case, the sidelobe level falls below -30dB at a relative spatial frequency s~1.4.

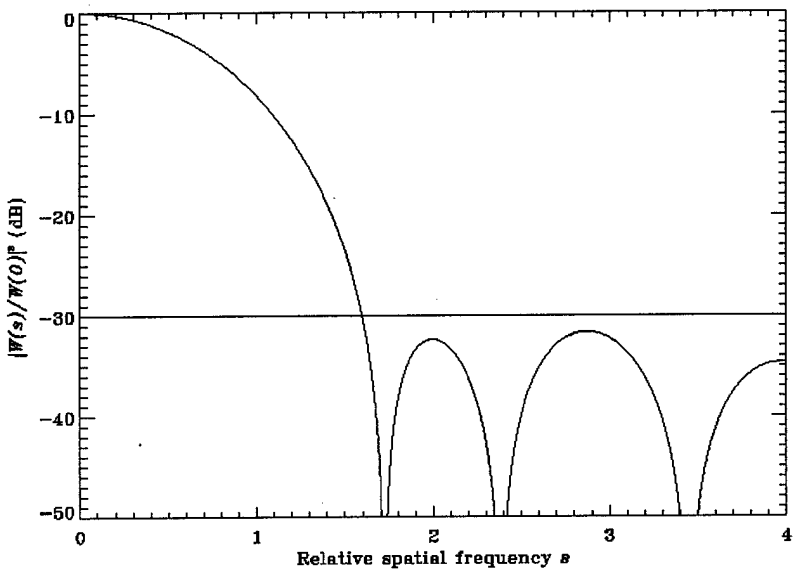

Figure 16 Bandpass of CBAOTF with Trapezoidal Window with β = 0.16

Several feasibility model CBAOTFs were designed, fabricated, and used in the experimental study on the bandpass response. The CBAOTF was a 45° CBAOTF in-line device using the internal mode conversion (IMC) arrangement.

Figure 17 shows the bandpass response of a tilted 45° TeO_2 CBAOTF. The bandpass response of this filter shows a suppressed sidelobe of 27dB at 3nm from the peak wavelength. There is a slight increase in the FWHM, to about 1.3nm.

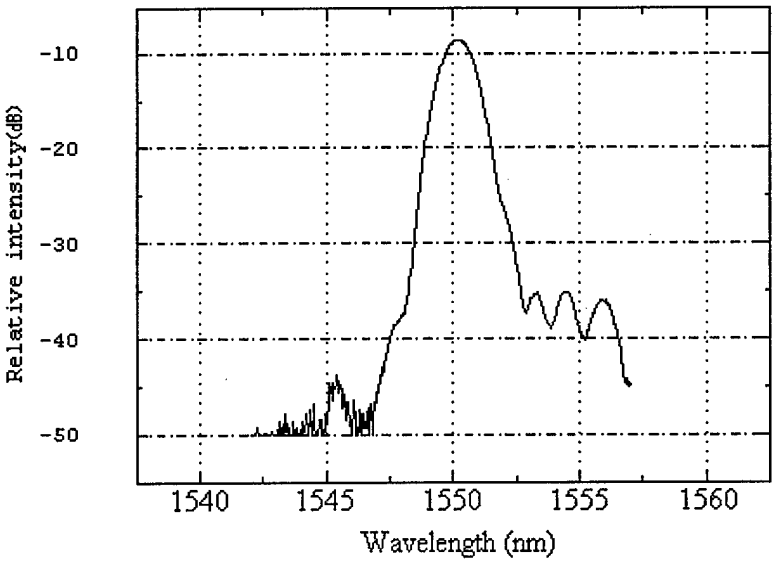

Figure 17 Bandpass of Tilted CBAOTF

Another technique for reducing the AOTF bandwidth and/or the sidelobe is to use two or more AOTFs in an incoherent optical cascade. The requirement is that the acoustic frequency shifts in the cascading AOTFs are the opposite, i.e. one up-shift and the other downshift. The bandpass response of the incoherently cascaded AOTFs is equal to the product of the single stage and thus can realize a significantly reduced sidelobe. The FWHM of the cascaded AOTF is also smaller. Since the frequency shifts are opposite for the two stages, the incoherent cascade offers the additional advantage of zero frequency shift.

Several pairs of TeO_2 CBAOTFs were designed, built and arranged in an optical cascade using a polarizer between the stages. The overall bandpass response of the cascaded device can be optimized by varying the chief ray directions. The bandwidths and sidelobe levels are summarized in Table 3-2

Table 3-2 Bandwidths and Sidelobes of Cascaded CBAOTFs

	Single Stage	Double Stage
Bandwidth	0.75nm	0.5nm
Sidelobe at -3nm	-28dB	-40dB
Sidelobe at +3nm	-22dB	-37dB

Figure 18 shows the experimental results of two cascaded CBAOTFs. At wavelength spacing greater than 1.6nm, the sidelobe level is -35dB below the central peak. Although a cascaded AOTF yields significantly lower sidelobes, the tradeoffs are increased construction complexity and doubling the drive power.

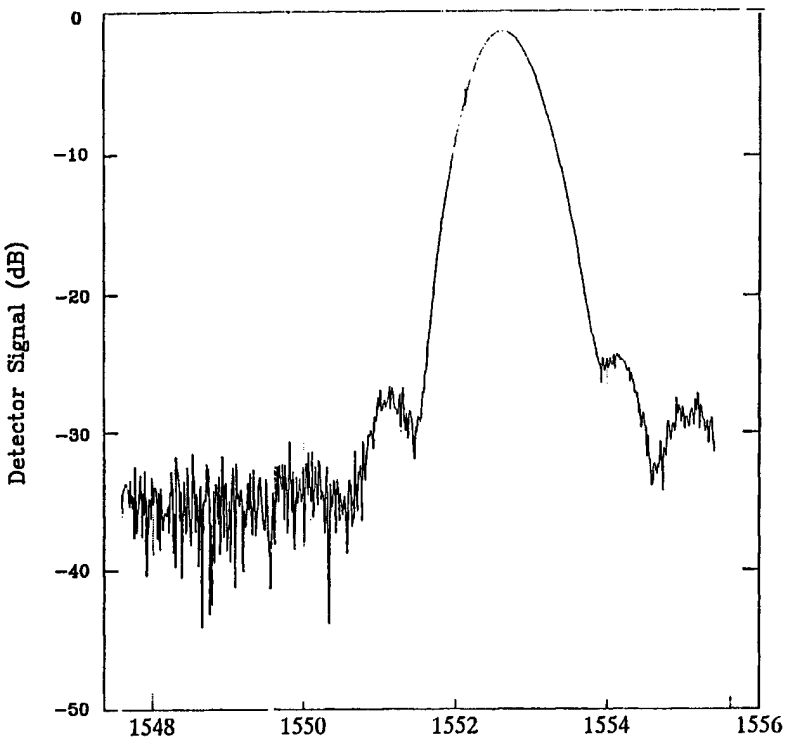

FWHM: 0.8nm, 20dB: 1nm, >1.6nm: 35dB

Figure 18 Bandpass of Cascaded CBAOTF

3.2 Reduction of Channel Spacing

The specified goal is to achieve 100GHz channel spacing. This corresponds to a wavenumber separation of $\Delta\sigma = 3.33\text{cm}^{-1}$. For the general case of an apodized AOTF, $\Delta\sigma$ at RdB is given by:

$$\Delta\sigma_R = \frac{k_R}{L\Delta n \sin^2\theta_o}$$

where L is the interaction length, θ_o is the polar angle of the optic axis and k_R is a parameter dependent upon the apodization and the specified RdB sidelobe level. For rectangular, triangular and Hamming windows, the values of R are given in Table 3-4 below.

Table 3-4 Values of k_R as a function of apodization window

R	Rectangular	Triangular	Hamming
-3dB	0.45	0.62	0.65
-30dB	9.5	1.4	1.76

The design goal is to achieve -30dB sidelobes at a 100GHz spacing (i.e., 0.8nm @ 1550nm): $\Delta\sigma_R=3.33\text{cm}^{-1}$. To meet this goal, the minimum crystal lengths L are calculated in Table 3-5 below.

Table 3-5 Selected Designs for Prototype CBAOTF (R=-30dB @ 100GHz)

Window θ_o	Triangular L (cm)	Hamming L (cm)
45°	6	7.6
55°	4.5	5.6
65°	3.7	5.0

The corresponding 3dB spectral width @ 1550 nm values are 0.6 and 0.7nm for triangular and Hamming windows, respectively. To keep the crystal length within practical limits, the polar angle θ_o for the optic axis is chosen to be greater than 55°.

To demonstrate the feasibility, a 65° prototype CBAOTF was designed, fabricated and tested. The measured results are as follows:

Measured Results of 65° CBAOTF

Acoustic Frequency:	50MHz
3dB Bandwidth:	0.5nm
Sidelobes @ 0.8nm:	24dB (R) 21dB (L)
@ 1.6nm:	27dB (R) 28dB (L)
@ 3.2nm:	33dB (R) 32dB (L)
Diffraction Efficiency:	90%
Drive Power:	80mW

Figure 19 shows the bandpass of the 65° CBAOTF.

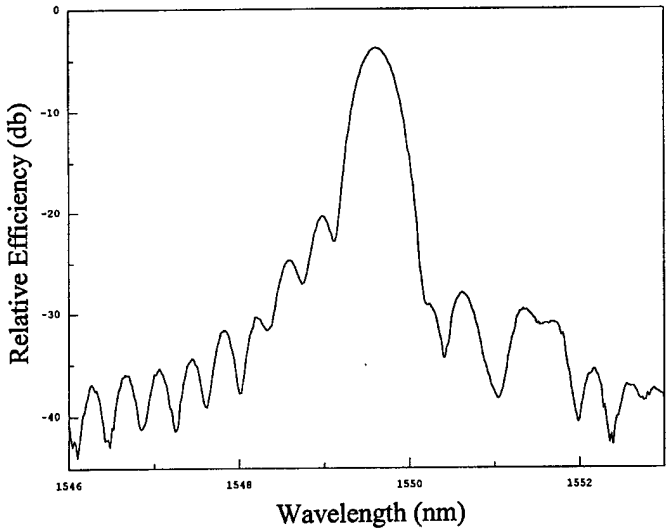

Figure 19 Bandpass of 65° CBAOTF

3.3 Improved Fabrication and Reliability

In the construction of AO-based dynamic WDM components, it was found that the major limitations of the AOTF are caused by (a) the inconsistent performance characteristics due to fabrication tolerances, and (b) the temperature dependent wavelength shift. These two critical issues are addressed below.

Orientation Tolerance

The CBAOTF uses a slow shear acoustic wave propagating of [110] axis with angle θ' in the (110) plane. For obtaining high resolution, α is a small angle, typically below 5°. Due to the large acoustic anisotropy of TeO_2, the acoustic beam walks off from the acoustic wave direction. Consider, for example, $\theta'=5°$. The angular sensitivity in the interaction plane is $\Delta\theta_r/\Delta\theta\approx 6$.

The angular sensitivity off the interaction plane is much larger. It turns out that the deviation of the acoustic beam angle $\Delta\phi g$ for a change of acoustic wave angle $\Delta\beta$ is given by $\Delta\phi g/\Delta\phi\approx 48$.

This puts a severe tolerance requirement on the x-ray orientation of the interaction plane normal. An orientation error of 5 minutes will introduce a deflection of the acoustic beam by 4° or a shift of 3mm. The acoustic beam will hit the side face and introduce a severe acoustic reflection problem. To keep the vertical shift less than 0.2mm, the orientation of the (110) plane must be accurate to within 20 seconds. This is not practical from a manufacturing point of view.

We propose to tilt the acoustic wave front away from the (110) plane, the off-axis angular sensitivity is then greatly reduced. For instance, at $\alpha=5°$, $\beta=5°$,

$$\frac{\Delta\phi_r}{\Delta\phi}=2.59 \qquad \frac{\Delta\theta_r}{\Delta\theta}=5.47$$

i.e. the angular sensitivity is reduced by a factor of 18.5. For the same requirement of 0.2mm error over 40mm acoustic beam path, (5 mrad. angular tolerance). The off-axis orientation accuracy can be as large as 6 minutes.

The figure of merit M_2 is about 4 times smaller than that of the conventional CBAOTF. This is the major disadvantage of the "tilted" CBAOTF.

Temperature Effect

Another key issue is the temperature-dependent wavelength shift. For the conventional CBAOTF where

$$\begin{aligned}\dot{c}_{44}&=-193.45\times 10^5\\ \dot{c}_{66}&=(877.3\times 10^5)\end{aligned} \quad \text{at } \theta'=5°,$$

$$\frac{1}{V}\frac{dV}{dT}=180\times 10^{-6} \text{ or } 180\text{ppm}/^\circ\text{C}.$$

For a CBAOTF operated at 1550nm, the wavelength shift $\delta\lambda$ is 0.28nm/°C. To keep the $\delta\lambda$ to within 10 percent of the FWHM for a CBAOTF with a FWHM of 0.5nm, the maximum temperature change is about 0.2 degrees. To operate the AOTF properly, active temperature tracking is required.

The temperature sensitivity can also be suppressed using the tilted CBAOTF. For the previous example, $\theta'=5°$, $\phi=5°$, $\frac{1}{V}\frac{dV}{dT}=19.4\times 10^{-6}/^\circ\text{C}$. The wavelength shift is reduced to 0.03nm/°C. For a maximum shift of 10 percent FWHM or 0.05nm, the device temperature needs to be maintained to within 1.7°C. Clearly, in this case no elaborate temperature control is necessary.

A design rule is developed based on the tradeoff between the angular and temperature sensitivity versus the diffraction efficiency and drive power. For a specific acoustic wave off-

axis angle α, these key parameters are calculated. The results for o=1550nm are shown below for these parameters, respectively: (Fig. 20) $\frac{d\theta_r}{d\theta}$, (Fig. 21) $\frac{d\phi_r}{d\phi}$, (Fig. 22) f, (Fig. 23) M_2, and (Fig. 24) $\frac{1}{V}\frac{dV}{dT}$.

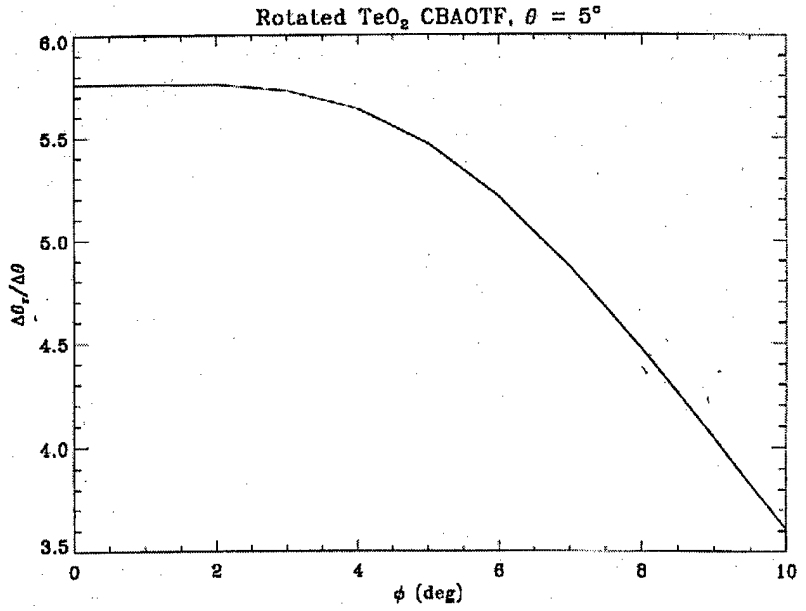

Figure 20 Plot of $\Delta\theta_g/\Delta\theta$ vs. Acoustic Wave Tilt Angle

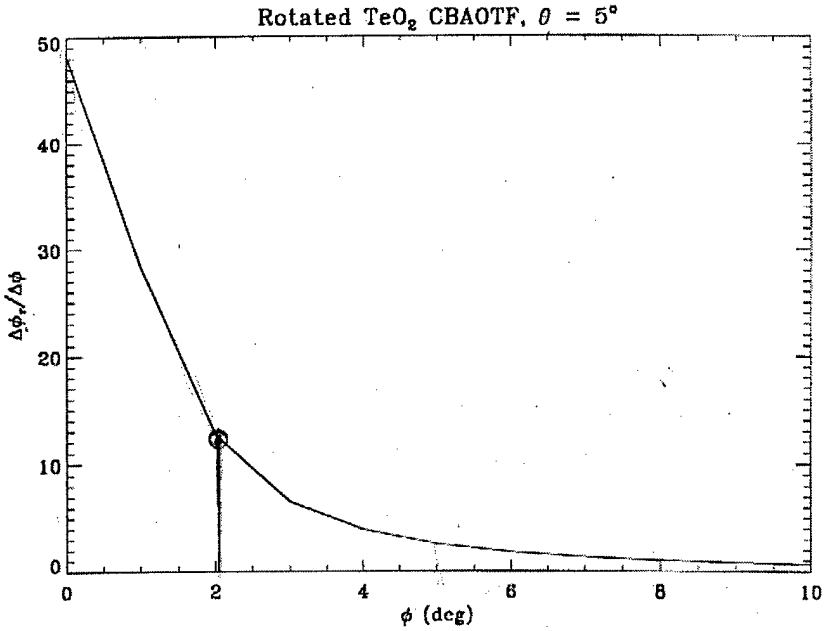

Figure 21 Plot of $\Delta\phi_g/\Delta\phi$ vs. Acoustic Wave Tilt Angle

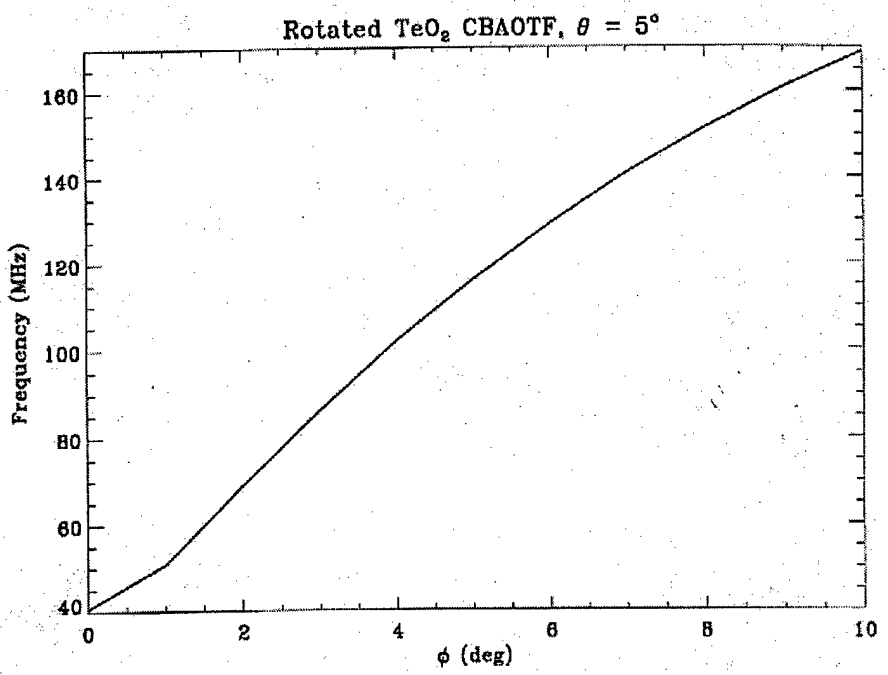

Figure 22 Acoustic Frequency of "Tilted" CBAOTF vs. Acoustic Wave Tilt Angle

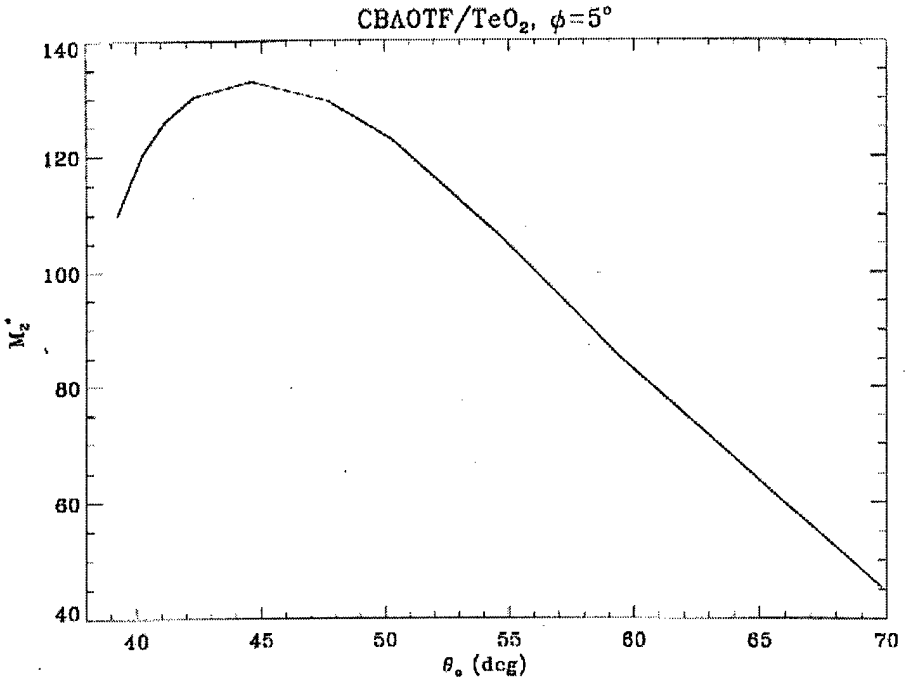

Figure 23 Plot of Figure of Merit vs. Optical Angle

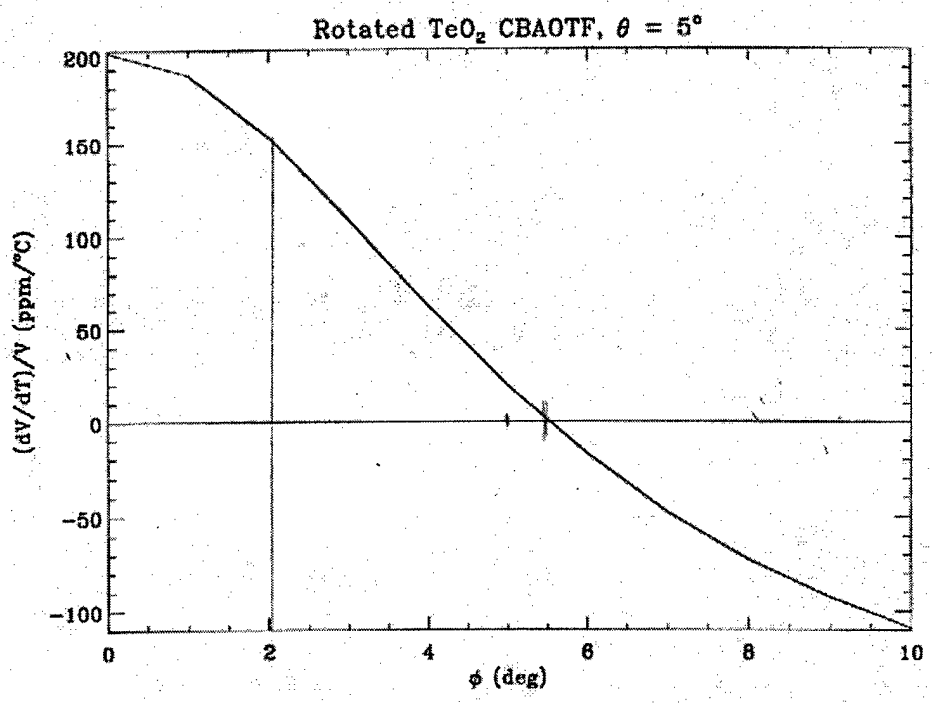

Figure 24 Plot of Temperature Sensitivity vs. Acoustic Wave Tilt Angle

4.0 Multi-Wave Optical Cross-Connect

For a narrowband optical filter, only one input and one output are needed. An AOTF can be configured as a 2x2 multi-wave OXC if the zeroth and first order ports are used both at the input and output end. To distinguish from the tunable filter type applications, the device will be referred to as an AOXC or AO switch (AOS). To implement a reconfigurable (R) OADM, an input Mux and an output Demux are needed.

Figure 25 shows the schematic of an ROADM based on the use of PIAOTF. Compared with the SDM implementation shown in Figure 4 (Section 2.1), a single 2x2 AOTF is equivalent to 32 sets of 2x2 switches and attenuators. For the implementation of a 2x2 OXC, the advantage of saving hardware is even more significant.

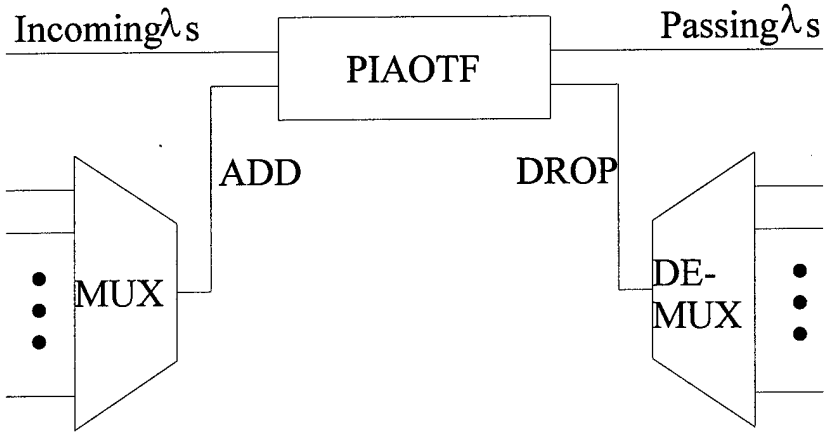

Figure 25 AO-Based Dynamic Optical Add & Drop Multiplexer

4.1 Critical issues of crosstalk

The most severe problem that limits the minimum channel spacing of an AO-based OADM or OXC is the signal degradation due to crosstalk. This section discusses the various types of crosstalk and approaches for reducing this deficiency. To be specific, the discussion of cross-reduction will be focused on 2x2 AO-based cross-connects.

4.1.1 Sources of crosstalk

There are three kinds of crosstalk, as described below:

(1) Sidelobes: The inter-channel crosstalk due to the interference at an adjacent wavelength with the selected signal is caused by the sidelobe level of the AOTF bandpass. The bandpass response of the AOTF is equal to the magnitude squared of the Fourier transform of the acoustic field distribution. A number of techniques for suppressing the sidelobes were proposed. With the use of apodized acoustic techniques, we have seen that the sidelobe can be suppressed to below 25dB. Furthermore, for OADM applications, this type of inter-channel crosstalk can be removed by the use of notch filters at the receiver end or the attenuators in the single wavelength channel after the passive Demux. Thus, except for very narrow channel

spacing below 0.8nm, the crosstalk due to sidelobe is less severe compared to other types of crosstalk.

(2) Extinction Ratio: This type of intra-channel crosstalk due to the finite extinction ratio of the AOTF is caused by the incomplete depletion of the zeroth order beam or the imperfect polarization ratio of the PBS. For the noncollinear type bulkwave AOTF, the finite leakage of the PBS is not an issue. However, due to the finite optical divergence of the optical beam, and incomplete polarization conversion of the AOTF, the AO diffraction is an analog process, complete depletion of the incident beam is not possible. Even with 98% efficiency, the residual optical power in the zero-order (undiffracted) beam still amounts to -17dB. Fortunately, this type is easily removable by the use of a space dilation architecture. High extinction ratio is obtainable if the output ports containing the undiffracted beams are terminated.

(3) Another intra-channel source of crosstalk is coherent intermodulation, which originates from the mixing of two collinearly propagating optical waves inside one wavelength channel [3]. For instance, when two acoustic frequencies, f_1 and f_2, corresponding to two adjacent laser wavelengths, λ_1 and λ_2 respectively, are applied, the diffracted light at λ_1 at the mainlobe and sidelobe will be frequency shifted by f_1 and f_2, respectively. The optical interference of the two light beams at λ_1 will result in an amplitude modulated type crosstalk at the difference frequency of f_1-f_2. This type of interchannel crosstalk is much more severe since the modulation is proportional to the amplitude or square root of the sidelobe power level. This type of coherent crosstalk is most difficult to suppress since the two interfering beams are diffracted from the same wavelength beam by multiple acoustic frequencies.

To reduce the critical performance degradation due to crosstalk, there are basically two approaches. One way is to modify the device design, for instance, by changing the interaction geometry or applying apodization to either acoustic or optical beams. This device-level approach is typically applicable to only one type of crosstalk. An alternative method is to use a system approach based on space dilation. Compared to the device-level approach, this approach is general since it is applicable to all types of crosstalk.

4.1.2 Crosstalk Reduction Architecture and Designs

This section discusses the architectures for reducing the crosstalk. Depending on which type of crosstalk is the dominant factor, there are several different preferred configurations. In the following discussion, single polarization filters (SPFs) with single polarized inputs are assumed since the o and e polarization can be handled by a parallel PDL configuration.

Fig. 26 shows the schematic of a space dilated 2x2 AOXC using two AOTFs in optical cascade. The first AOTF and the second AOTF function as an add filter and a drop filter, respectively. They are both driven by the same wavelength selecting frequency f_A. In the first cell, the first order crosstalk (e.g. the sideband) terms in the "drop" terminals. A'_1 and A'_2 are on the order of δ. Similarly, B'_1 and B'_2 are of order ε, which is the diffraction efficiency at the sidelobe wavelength, are the "left over" terms due to incomplete dilation of order $\delta = 1 - \eta$. Both these optical beams are diffracted again in the second "add" AOTF. Thus, the sidelobe and "left over" terms at the output terminals 1' and 2' are of second order ε^2 and δ^2. Based on this scheme, in order to achieve a total crosstalk under 25dB, the contribution due to sidelobe and incomplete

depletion for each AOTF must be reduced to below 12.5dB, which is significantly easy to satisfy.

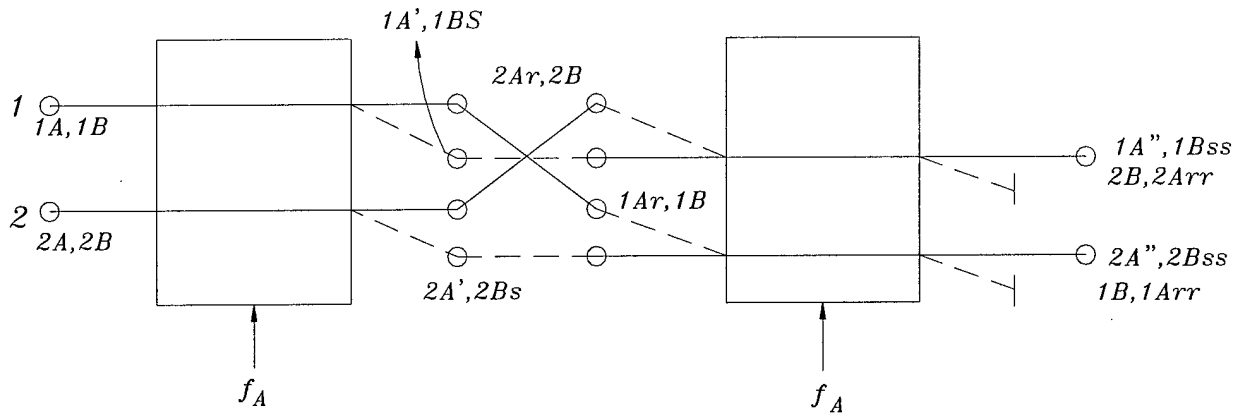

Figure 26 Space Dilated 2x2 AOXC using two AOTFs in optical cascade

Figure 27 shows a different arrangement for the space dilated AOXC. The first cell is the same as in the previous arrangement and is driven by the wavelength selecting frequency f_A. The second "add" cell is now driven by the "complementary" frequency f_B. The interconnecting beams between the two AOTFs are arranged so that final outputs are of order $\varepsilon\delta$. This arrangement is, in general, better than the first when the two types of crosstalk are not equal. It is particularly advantageous to bulkwave configuration since the crosstalk term due to incomplete depletion is more severe. For AOXC, the crosstalk due to finite extinction ratio is a more severe contribution.

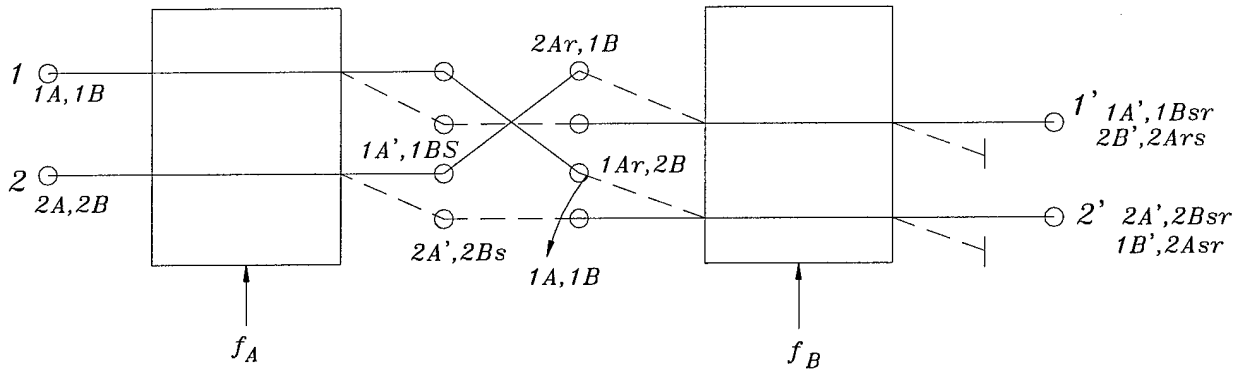

Figure 27 Alternate Arrangement of Space Dilated AOXC

The use of apodization could effectively reduce the sidelobe levels. As a result, for a bulkwave AOXC, the dominant crosstalk contribution is due to incomplete depletion or the low extinction ratio of the undiffracted beam. Figure 28 shows the schematic of a high extinction AOXC using a pair of AOTFs in optical cascade. In this case, devices 1 and 2 serve as "drop" and "add" cells, respectively. Notice that all the optical beams reaching the final output must be diffracted at least once. Thus, extremely high extinction ratio is obtainable.

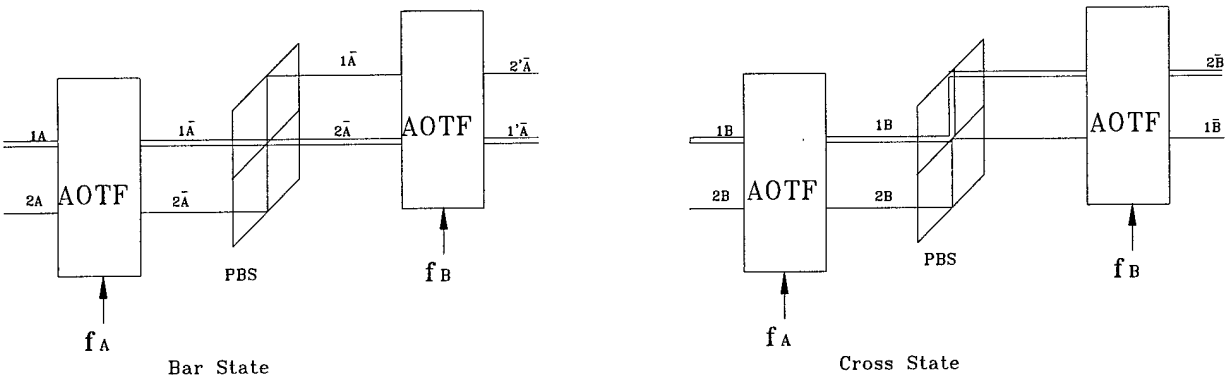

Figure 28 High Extinction AOXC

The space dilated AOXC discussed above can be constructed either in an in-plane or dual parallel plane along the height direction. The two configurations differ on how the beam exchange interconnection occurs, horizontally (in the interaction plane) or vertically (between the two parallel planes). It will be seen that the parallel plane configuration has the advantage of providing additional flexibility for realizing wavelength dilations.

The crosstalk reduction design described above are not effective for the coherent crosstalk generated by the application of single acoustic wave with two acoustic frequencies. To suppress the coherent crosstalk, the use of multiple acoustic waves is required.

Figure 29 shows the schematic and the associated wavevector diagram of the twin-channel AOTF. Two transducers are bonded to the SPF that generates two acoustic waves with slightly different acoustic wave directions that correspond to the odd and even wavelength channels, respectively. The twin-channel AOTF thus provides a wavelength-dilated structure that suppresses coherent crosstalk.

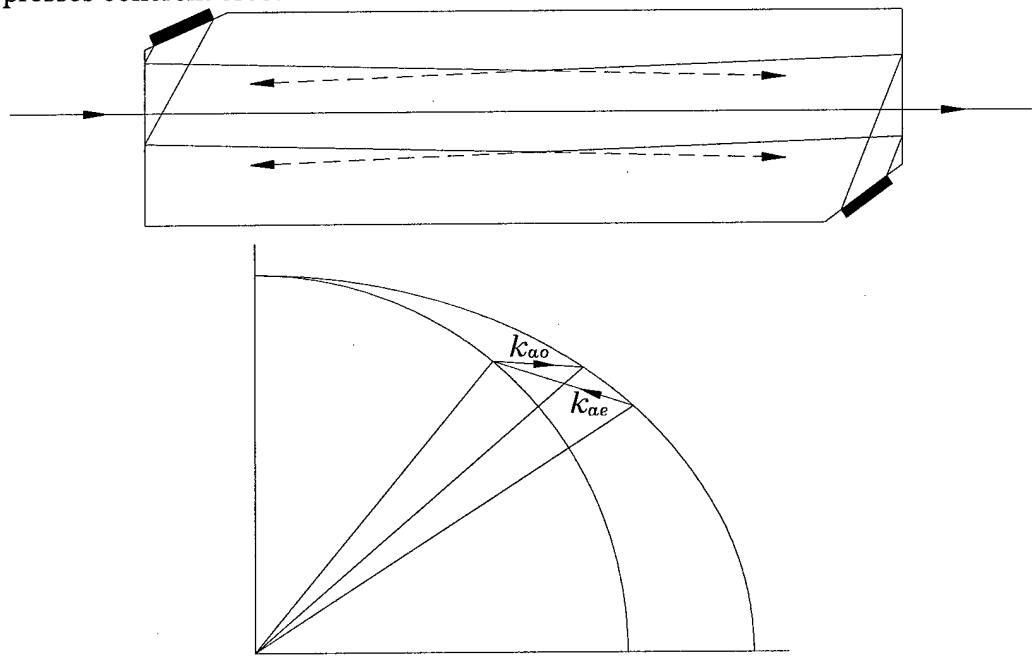

Figure 29 Configuration and wavevector diagram of Twin-Channel AOTF

Also shown in Figure 29 is a wavevector diagram of AO diffraction from two acoustic waves for the selection of two neighboring channels. For instance, wavevector $\bar{k}_{ao}$ and $\bar{k}_{ae}$ are chosen for the selection of odd and even channels, respectively. To maintain the interaction length, the width of the acoustic wave should be sufficiently wide so that most of the optical beam overlaps both of the acoustic beams.

Figure 30 shows the wavevector diagram of another AOXC using two acoustic waves. Two axial symmetrically acoustic waves are launched in the TeO_2 crystal, from a planar phased array transducer. A pair of polarized input optical waves is diffracted by the AO cell. The bar state optical beam coupling that occurs when the excited acoustic frequency f_b and the selected wavelengths λ_b satisfy the phase matching condition. Similarly, coupling occurs for the cross state when the AO cell is driven by f_c. In both cases, the zero-order optical waves are terminated and the two output optical beams for both the bar and the cross states are first order diffractions Thus, high extinction ratio is expected for the single stage dual mode.

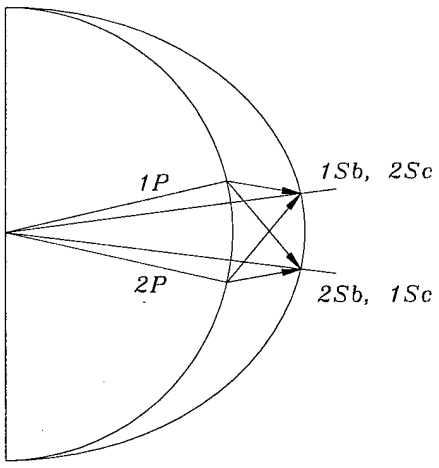

Figure 30 Wavevector diagram of 2x2 High Extinction AOS

4.2 2x2 AOXC Experiments

To verify the crosstalk reduction techniques, a feasibility demonstration model 2x2 AOXC was designed and constructed [11]. For simplicity, single polarization AOTFs (SPFs) with single polarization inputs are used since the PI version can be easily constructed using the PDL configuration.

Bypass and Exchange Beamformer

In the construction of a low crosstalk AOXC using dilation structures, there is a need to bypass or exchange output ports between the cascaded stages of the AOTFs. There are a number of physical implementations for realizing the bypass-exchange function for interconnecting AOS in a dilated configuration. The proposed approach is to use a polarization interconnection (POI) module composed of PBS arrays or ordinary reflectors (mirrors). The PBS implementation allows design flexibility for matching to the input or output optical beams with either small or large spatial separations. Figure 31 shows, for example, the interconnection matrix and the physical implementation of a particular stage of POI module. By choosing the mask design for depositing ordinary polarization transmission and reflection grids, the optical exchange matrix

corresponding to any specific Benes network pattern can be readily realized using conventional thin film coating techniques.

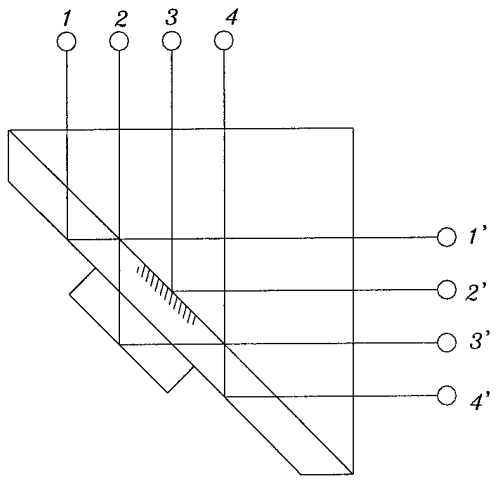

Input	Output
1	1
2	3
3	2
4	4

Benes algorithm

Figure 31 Interconnection Matrix

Selection of Dilation Architecture

The objective of the demonstration model is to examine the effectiveness of dilation in reducing the crosstalk. Prior to the experimental work, the dilation architectures shown in Figures 26 to 28 must be examined in more detail. There exists a basic tradeoff between the two types of crosstalk due to sidelobes and extinction ratio. To increase the extinction ratio, the AOTF must be driven into a nonlinear region. This will increase the sidelobes. On the other hand, operation of the AOTF at lower efficiency will certainly lower the extinction ratio. For a near linear operation, the peak efficiency needs to be reduced to below 70 percent. As a result, the dilation structure such as the one shown in Figure 26 must be eliminated. It is clear that at least for the bulkwave AOTF, the selected output optical beam must be diffracted at least once in passing through the cascaded cells.

In addition to high sidelobes, the operation of the AOTF in the high efficiency region has other important disadvantages. These include high drive power and thermal degradation, reduction of SMF coupling efficiency due to wavefront distortion, and most severely, the large increase in coherent crosstalk due to intermodulations. As a first basic guideline, it is important to operate the AOTF in the linear efficiency region for the diffracted light.

To insure low crosstalk due to incomplete depletion, the zeroth order beam needs to be efficiently diffracted but not to the same first order. To achieve this goal while maintaining the linear operation, a second guideline is to use an acoustic beam with larger acoustic divergence than the optical divergence, or $\delta\theta_a > \delta\theta_o$. The net result is an increased "suck out" efficiency for the undiffracted beam. The increase of divergence ratio also has the advantage of reducing coherent crosstalk.

Based on the above discussion, the high extinction cascaded configuration shown in Figure 27 or 28 are chosen for the demonstration model experiment.

Experimental Results of Dilated AOXC

Figure 32 shows the optical configuration of the demonstration model AOXC. It consists oc two optically cascaded CBAOTFs and bypass/exchange beamformers integrated into an

optical bench. The two AOTFs are driven by two separate multi-frequency RF signal sources such as Direct Digital Synthesizers (DDS). Due to the relatively low frequency for driving the AOTF near 1550nm (about 50MHz), the low-cost DDS synthesizers presently available (with a typical clock rate of 300MHz) will not produce harmonic distortion and easily meet the requirements.

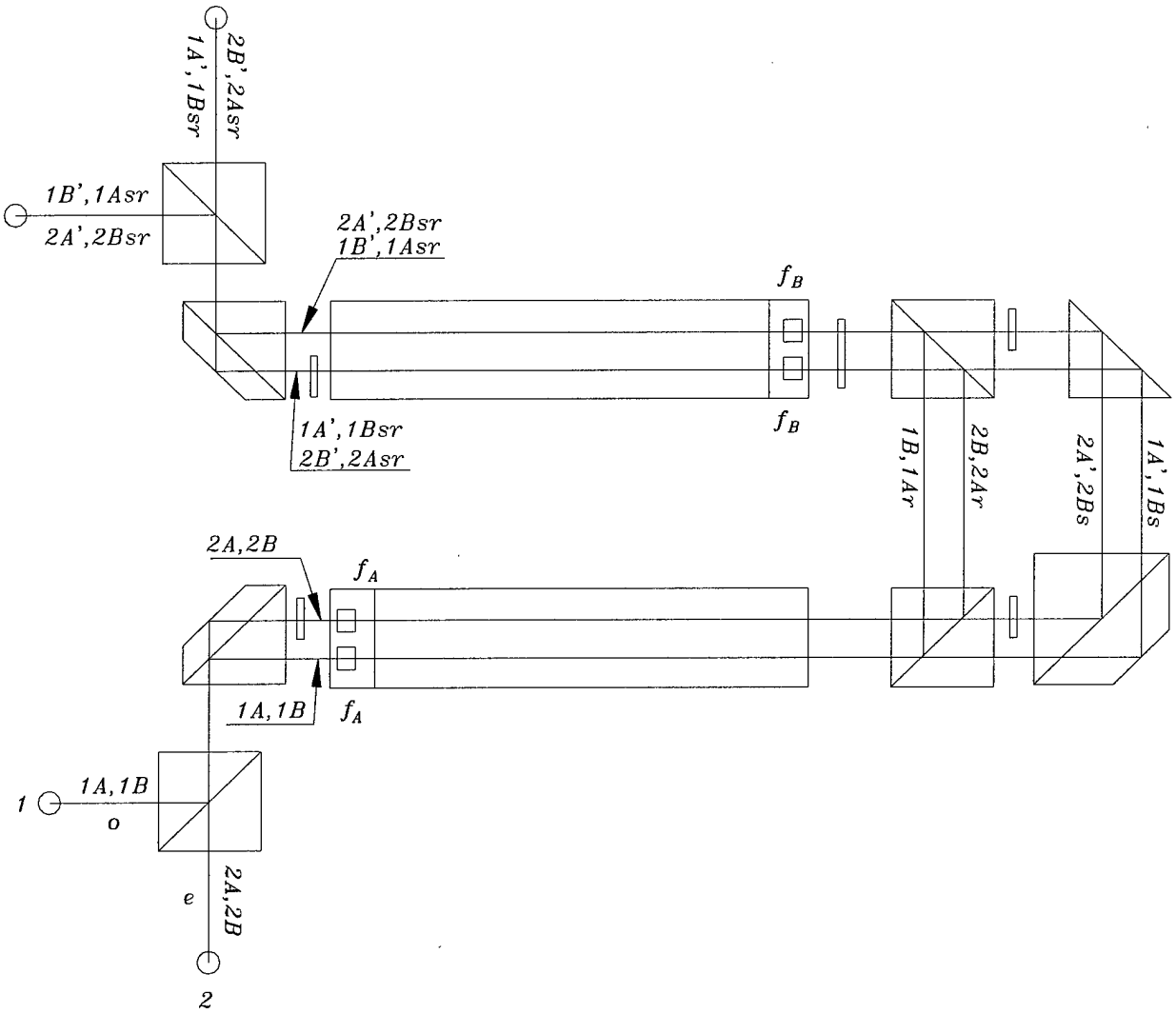

Figure 32 Demonstration Model AOXC

A cascaded two-stage CBAOTF using the space dilation structure was constructed as the demonstration model (DEMO). Test results of the DEMO are summarized in Table 4-1. The experiment was performed using a single laser source with two separate acoustic signals. Thus, the measured results represent the worst type of crosstalk, i.e., the coherent type due to interchannel intermodulation products.

Table 4-1 Measured Results of Dilated AOXC

	First AOTF	Second AOTF	Cascaded
Bar State Loss (depletion)	14dB	15dB	>30dB
Cross State Loss (sidelobe)	17dB	16dB	>30dB

As shown in Table 4-1 above, at the channel spacing of 1.6nm, the crosstalk level due to sidelobe and extinction ratio for the dilated two-stage AOTF are both under -25dB. The FWHM of the cascaded AOTF is about 0.5nm. Figure 33 shows a photo of the demonstration model.

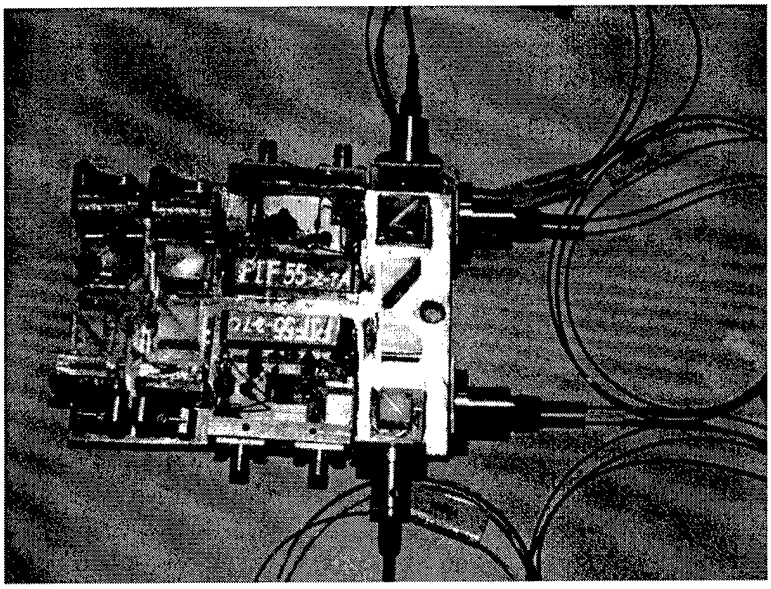

Figure 33 Demonstration Model Dilated AOXC

5.0 Dynamic Fiber Amplifier Equalizer

The widespread use of Erbium Doped Fiber Amplifiers (EDFA) has extended the range and increased the capabilities of optical fiber communications. However, with the need for larger bandwidth, these amplifiers are being used more and more in WDM systems. Because the gain of these amplifiers depends strongly on wavelength and input signal size over the 1525-1570nm band used for WDM channels, the reliability of WDM systems can be threatened by wide variations in signal size between WDM channels. Because a PIAOTF can be operated as a programmable WDM attenuator, these wide variations in channel to channel signal size can be corrected dynamically.

The DFAE has many advantages over passive gain flattening filters. Because it is dynamically controlled, it can respond to gain changes and correct them. The passive filter is designed to correct for only one gain curve, while the DEFA can be programmed to correct for any gain profile (for example the profile from a group of cascaded EDFAs). Therefore, networks utilizing both DFAE and ordinary EDFA would require fewer gain-correcting elements. If the network developed a gain instability lasting more than a few seconds, the DFAE would automatically damp the gain fluctuation.

5.1 System Architecture

The basic design of this amplifier system is shown in Figure 34. The amplifier achieves high gain through a cascaded design of two EDFA with the AOTF centered between them. This also eliminates some sensitivity of the system to the insertion loss introduced by the PIAOTF. For the prototype phase of the product these amplifiers will be stand-alone bench top EDFA. In the final product design, the EDFA and AOTF will be contained in the same enclosure.

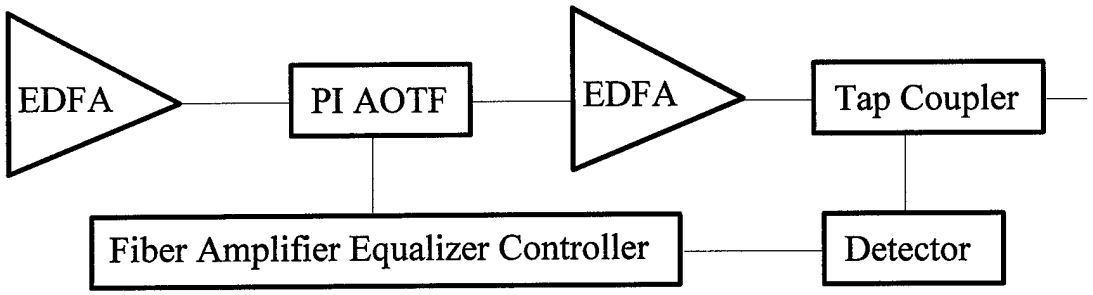

Figure 34 DFAE Basic Configuration

Operation of the AO based DEFA is based on the intrinsic capability of the AOTF to simultaneously and independently control the multi-wavelength signals passing through it. The key issue is that in order to exercise the feedback control; it is necessary to detect the amplitude of each signal.

The use of wavelength de-multiplexer control is illustrated in Figure 35. Multiple wavelengths are first amplified by the EDFA and then passed to the AOTF equalizer, which is driven by an RF sum signal containing the component frequencies necessary to produce the required spectral bandpass channels. A small fraction of the equalizer output is sampled through an optical directional coupler and spectrally decomposed and detected. These signals are used as input to the control loop, which continually adjusts the individual RF levels to maintain each wavelength channel at the desired level. Detection of the sampled power spectra is performed after the multi-wavelength output is channelized by a passive WDM Demux.

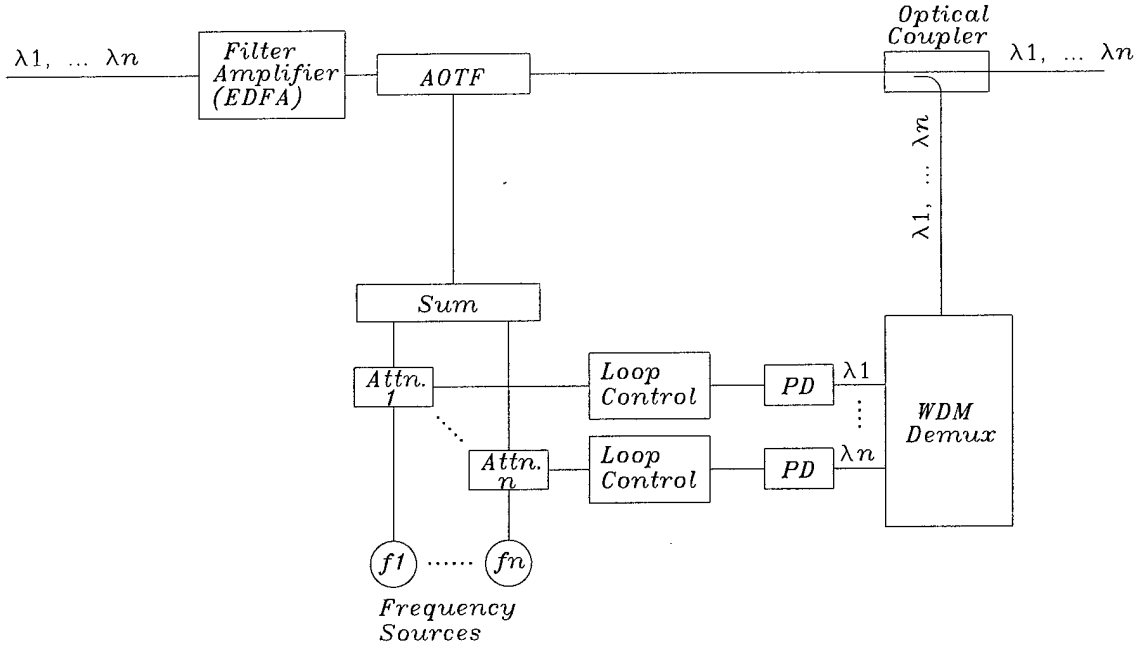

Figure 35 Basic Wavelength Demultiplexer Control Approach

Operation of the AO-based DFAE is explained as follows: Multiple wavelengths are first amplified by the EDFA and then passed to the AOTF equalizer, which is driven by an RF sum

signal containing the component frequencies necessary to produce the required spectral bandpass channels. A small fraction of the input beam is used as the monitoring beam, which is sampled through an optical directional coupler and passes through the AOTF in a spatially separate channel. The first order diffracted signal of the monitoring beam is detected and used to set the RF power control to continually adjust the individual RF levels to maintain each wavelength channel at the desired level.

The basic approach for implementing the DEFA shown in Figure 36 above requires the use of a set of passive DWDMs, N parallel channels of detectors and feedback control electronics. This increases the total size, complexity and cost of the overall system. In the sections to follow, an all AO approaches for the DFAE are discussed.

Consider the basic architecture of the DEFA. The following configurations are considered.

- Separate AOTFs that serve as a programmable multi-wave attenuator (MWA) and a WDM spectrum monitor
- Single AOTF that serves as MWA and the WDM monitor

Use of Separate Monitoring AOTF

The use of a second AOTF to monitor the amplitude of each wavelength is an alternative approach. Compared to the passive DWDM channelization scheme, the use of a WDM monitoring AOTF has the advantage of being a simple, flexible low-cost option. In addition to detecting the amplitude, this approach also provides the wavelength or optical spectrum as well. Figure 36 shows the block diagram of this AOTF monitoring scheme.

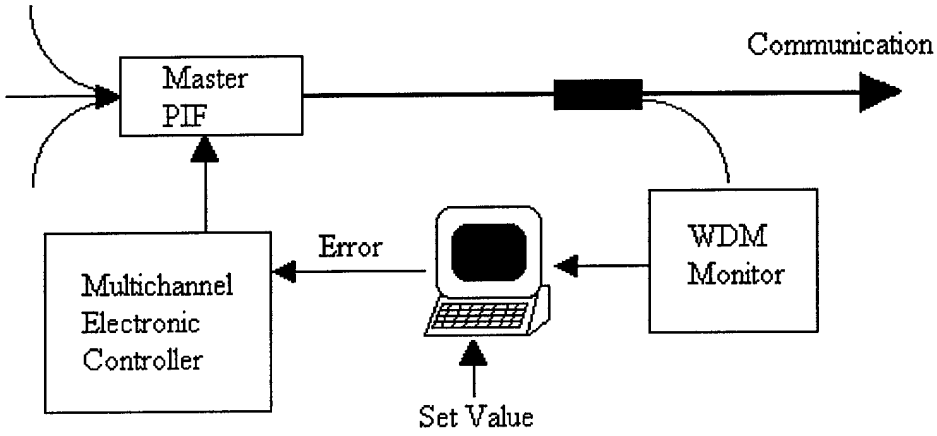

Figure 36 DFAE using a Separate Monitoring AOTF (WDM Monitor)

The use of a separate monitoring channel AOTF to monitor the amplitude of each wavelength has the advantage of being a simple, flexible low-cost option without intrusion on the DWDM communications. In addition to detecting the amplitude, this approach also provides the wavelength or optical spectrum. Thus, not only is this monitoring needed for the DFAE for its automatic gain correction, it also serves as a continuous monitor of the signal size in each WDM channel and therefore can be used as a diagnostic of network health at an in-line location.

A very important advantage of the DFAE approach over the passive flattening approach is that not only is this monitoring needed for the DFAE for its automatic gain correction, it also serves as a continuous monitor of the signal size in each WDM channel and therefore can be used as a diagnostic of network health at an in-line location. This monitoring is done with a single tap coupler (1%) and a single photodiode and does not require an expensive WDM communication band. Instead, a single photodetector is used and channel identification is achieved by very small, non-intrusive unique channel modulations introduced by the equalizer control electronics. The entire equalizer block optics and electronics can be integrated into a single compact module.

Single AOTF-Based DFAE System

Instead of using two separate units, a single AOTF can function as both the programmable multi-wave attenuator (i.e., the multi-wave AOTF) as well as the monitoring AOTF. This scheme uses one AOTF, thus simplifying the complexity of interconnecting optics and lowering the cost of the system. The major disadvantage is that the operation may intrude on the main line of the operation of the communication system.

Figure 37 shows the basic structure of the single-AOTF automatic gain control (AGC) DEFA. The zeroth order beam is used to adjust he amplitudes of the multi-wavelength signals while the first order deflected beam is used to monitor the optical spectrum. Besides simplicity, one practical advantage of this scheme is that the closed-loop feedback signal is derived from the same AOTF using a two-level modulation scheme, thus eliminating the need for accurate calibration between the two AOTFs (e.g., temperature drift). The major disadvantage of this scheme is that the main communication channel may be intruded upon and thus causing system degradation. This problem may be eliminated by electronic filtering at the output end. Since the frequency of the low-level modulation is fixed and low frequency (typically below 10KHz), it should be eliminated at the output with narrowband rejection filters. Nevertheless, this is a system issue that needs to be resolved.

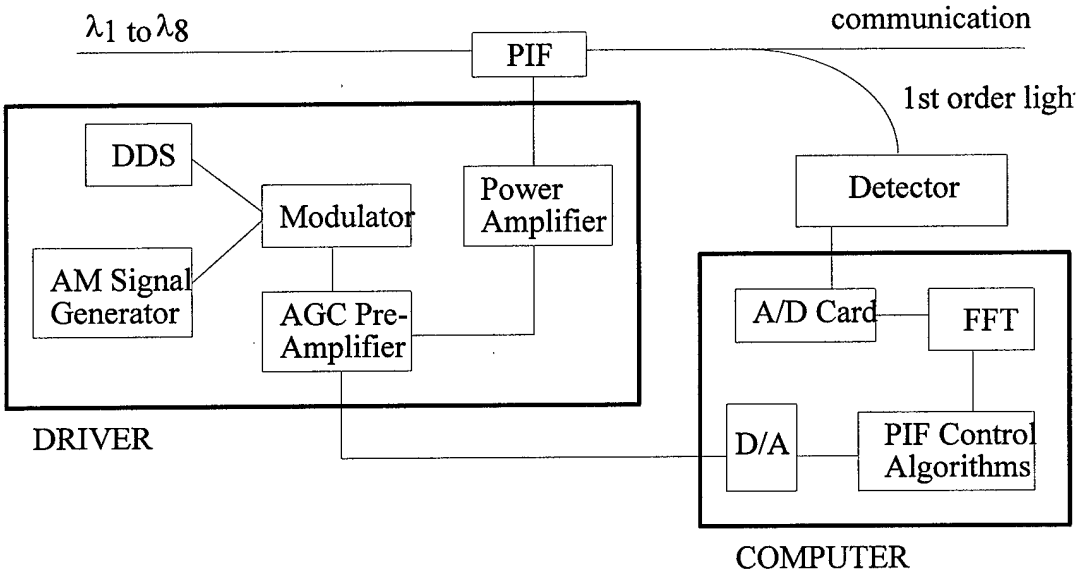

Figure 37 DFAE configuration using single AOTF

An alternative approach for realizing a non-intrusive DFAE is to implement the monitoring AOTF in a spatially separate channel of the MWA AOTF. As shown in Figure 38, the first order beam is detected and used to set the RF power control.

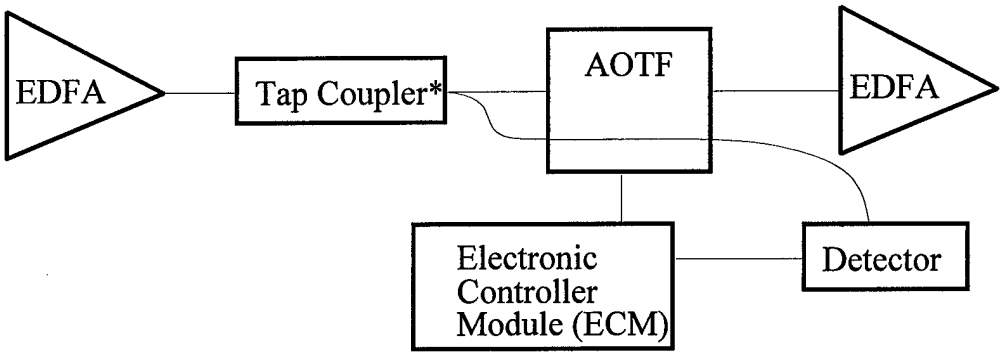

Figure 38 Alternative DFAE configuration using single AOTF

5.2 Modulation Decoding Scheme

Using either of the two types of DFAE architecture, the issue of how to acquire the amplitude information of different wavelengths must be addressed. This is discussed in this section.

Scanning Modulation Mode - A simple method is to scan the AOTF over the ITO grid of the WDM spectrum. The use of separate monitoring AOTF is particularly simple. The relative amplitudes of multi-wavelength laser lines (measured in dB) are determined. This is later used to set the (relative) RF power into the master AOTF in order to achieve dynamic equalization. In the case of the single AOTF-based DFAE, the RF is scanned with an incremental increase or amplitude modulation over the optical spectrum. The change of RF power required for each channel is also determined.

The simple sequential tuning or scanning method avoids the problems caused by crosstalk (e.g., sidelobes or frequency mixing) and provides the most unambiguous readout of the optical spectrum. The major drawback of this approach is the limited scanning speed. Typically, the random access time per resolution spot of the AOTF is about 50μsec. To apply an oversampling (e.g., 10 times the mode spacing or 0.08nm for a WDM spectrum with 100GHz spacing), the time for sweeping across 16 channels requires 160 x 50 = 0.8msec. For most practical situations, this is entirely acceptable.

The "Low Level Amplitude Modulation (AM) Decoding" approach shown in Figure 39 eliminates the need for wavelength de-multiplexing in the monitor control loop and requires only a single photodiode monitor. Each entering wavelength carrier is uniquely AM modulated at a low level by an identifier frequency M inside the AOTF. The composite intensity modulation is monitored by a single photodiode, which provides a composite signal containing M_1 through M_N signals, is extracted by a coherent detection (lock-in detection) approach using the original M_N modulator source as a reference. Since the detected level of M_N is proportional to the λ_N carrier level, this signal provides an error control for maintaining the desired λ_N output level.

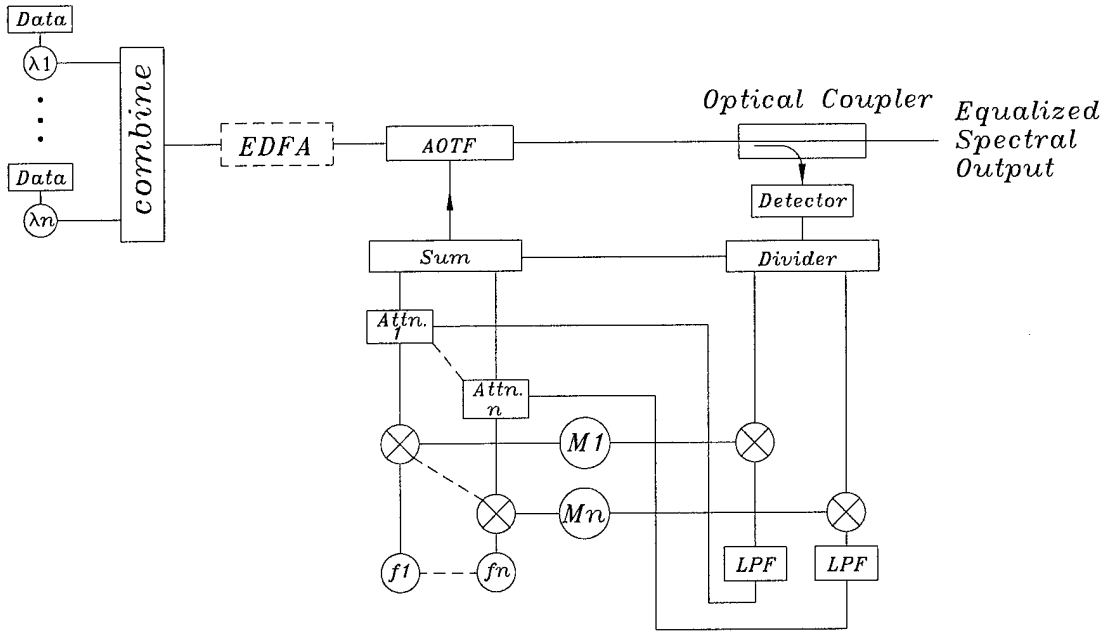

Figure 39 Low Level AM Modulation Encoding

In the above AM decoding scheme, the modulation is derived from modulating the driven (acoustic) waves inside the AOTF. Another approach uses the amplitude subcarrier modulation scheme shown in Figure 40. In addition to the data stream, the individual laser diode transmitter prior to the WDM Mux also transmits a subcarrier pilot tone. Each subcarrier AM frequency is chosen to be f_k (k=1, ...N), which is equal to the sum of the acoustic frequency driven by the optical carrier inside the AOTF at wavelength λ_k and a common local oscillator at frequency f_{LO}. At the AOTF end, the optical subcarrier is extracted by a single photodetector and a filter bank. The detected subcarriers are down-converted to f_k to be used for driving the AOTF. The spectrum of the subcarrier is detected and is used to set the desired attenuation to achieve the gain equalization. Notice the subcarrier decoding scheme is a more general system approach that can be used as a pilot-tone header to decode other information; e.g., as a method to implement self-routing of optical signals.

One approach uses the amplitude subcarrier modulation scheme shown in Figure 40. In addition to the data stream, the individual laser diode transmitter prior to the WDM Mux also transmits a subcarrier pilot tone. Each subcarrier AM frequency is chosen to be f_k (k=1, ...N), which is equal to the sum of the acoustic frequency driven by the optical carrier inside the AOTF at wavelength λ_k and a common local oscillator at frequency f_{LO}. At the AOTF end, the optical subcarrier is extracted by a single photodetector and a filter bank. The detected subcarriers are down-converted to f_k to be used for driving the AOTF. The spectrum of the subcarrier is detected and is used to set the desired attenuation to achieve the gain equalization.

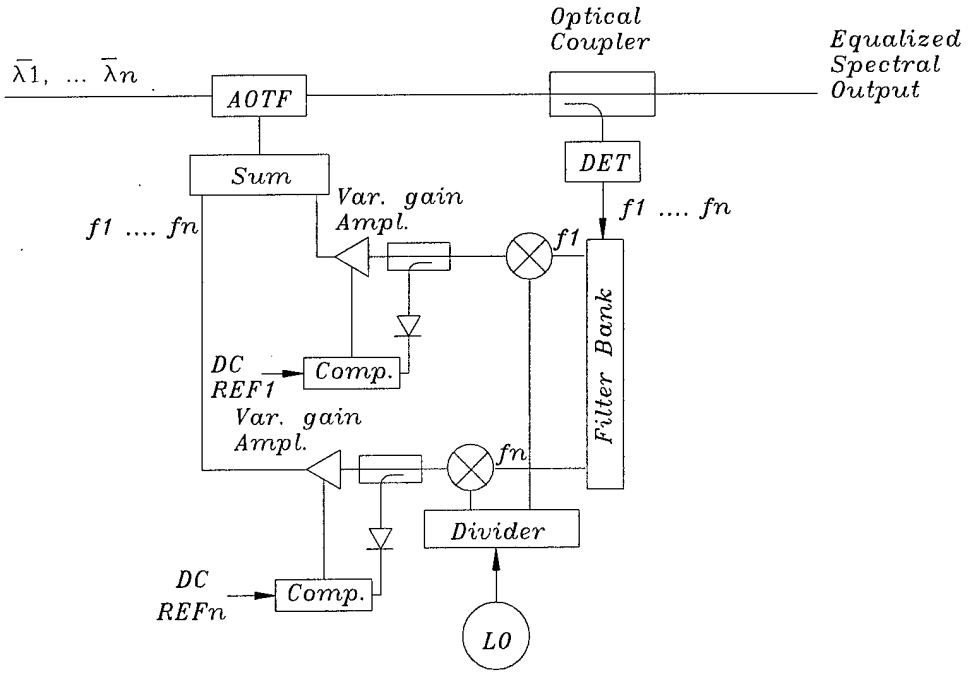

$\overline{\lambda}_n$ indicates that the wavelength has subcarrier modulation frequency f_n.

Figure 40 Subcarrier Modulation Decoding

In the "Intrinsic Coherent Decoding" approach (shown in Figure 41), the need for low level identifier modulation is eliminated. Each wavelength carrier passing through the "filtered" 1st order branch has an intrinsic small wavelength shift corresponding to the associated RF drive frequency f_N.

By coherently combining a sample of the filtered port with a sample of the input and detecting the optical sum with the photodiode, a heterodyne signal at f_N is generated as an output.

The multiplication correction can be done at any convenient point after extraction of the heterodyne signal by coherent (lock-in) detection identical to that described earlier. The power level maintaining control loop then uses the $P_{N(OUT)}$ to create an error signal for operation.

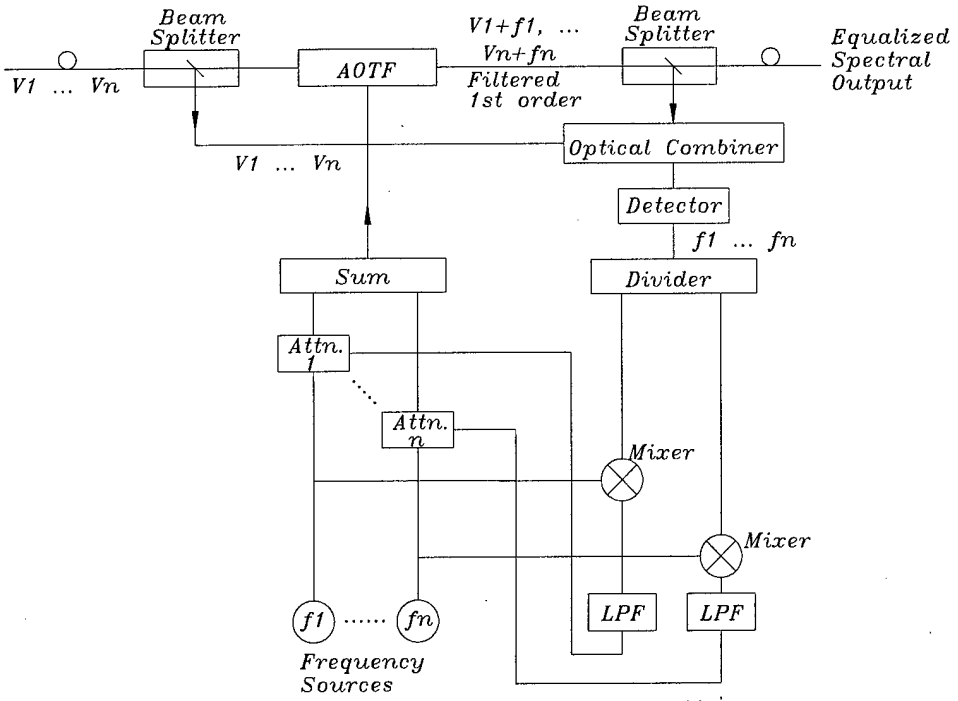

Figure 41 Intrinsic Coherent Decoding

5.3 DFAE Demonstration Model

In order to verify the feasibility of the AOTF –based DFAE, a demonstration model shown in Figure 36 was constructed. The DFAE system includes a master AOTF that serves as a multi-wave programmable attenuator (MPA), a second AOTF used as a WDM monitor, and a multi-frequency driver/controller. The use of the separate monitoring AOTF was chosen since it provides operation flexibility without causing intrusion to the optical signals passing through the MPA. Figure 42 shows a photograph of the Demonstration Model DFAE.

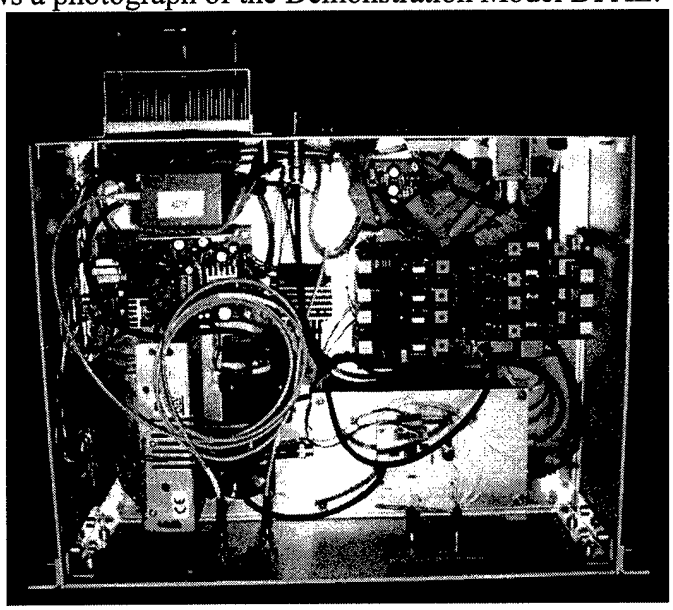

Figure 42 Demonstration Model DFAE

The AO-based DFAE can be operated either in the bar state depletion mode or in the cross state filtered mode. The bar state operation has the advantage of smaller optical insertion loss and lower drive power. On the other hand, the cross state filtered operation can achieve higher dynamic range and has the significant advantage of suppressed noise from the amplified spontaneous emission (ASE).

Prior to the test of the DFAE, the performance of the WDM monitor was tested. The monitor was constructed using a dual-polarization AOTF. To operate in the PI mode, both the p and s components of the filtered light are focused to a single detector. Figure 43 shows the tuning curve for the electronically summed PIAOTF or EPIF at room temperature.

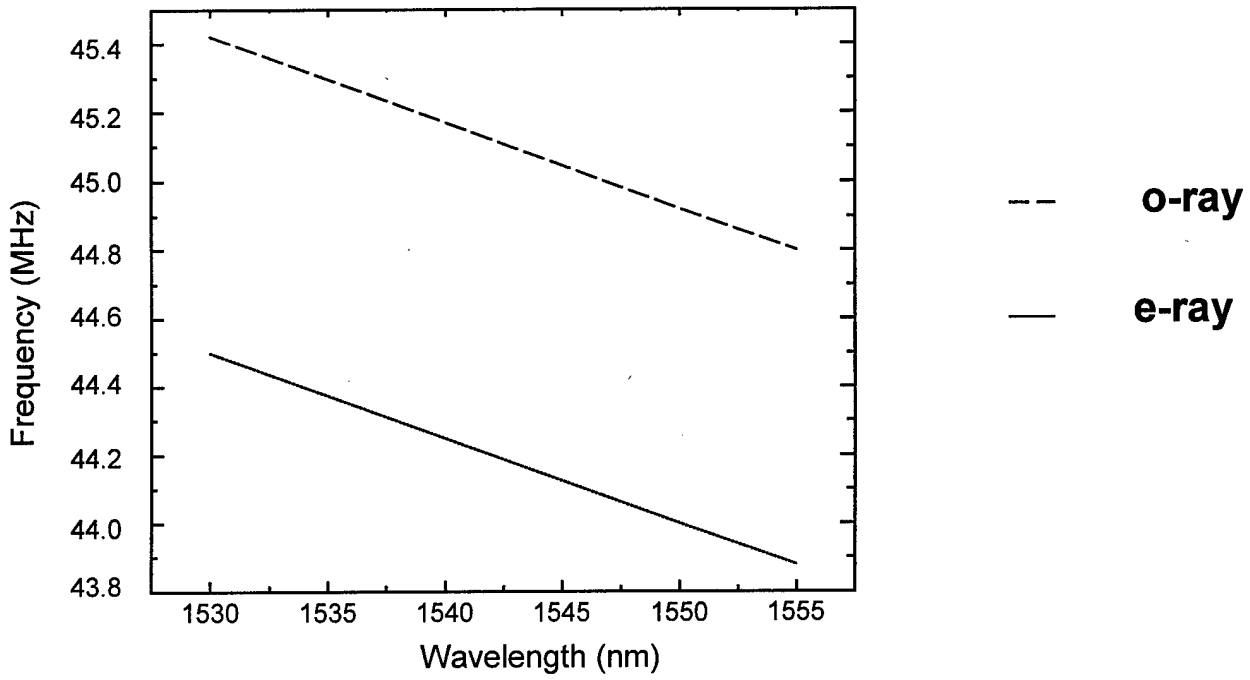

Figure 43 Measured Tuning Curve of EPIF

A series of measurement of the EPIF were made in order determined the temperature dependence. Figure 44 shows the measured frequency as a function of the temperature. The measured results indicate a wavelength shift of 0.17 nm per degree or equivalently 110ppm/°C. To reduce the temperature sensitivity, suitable temperature feedback control is required.

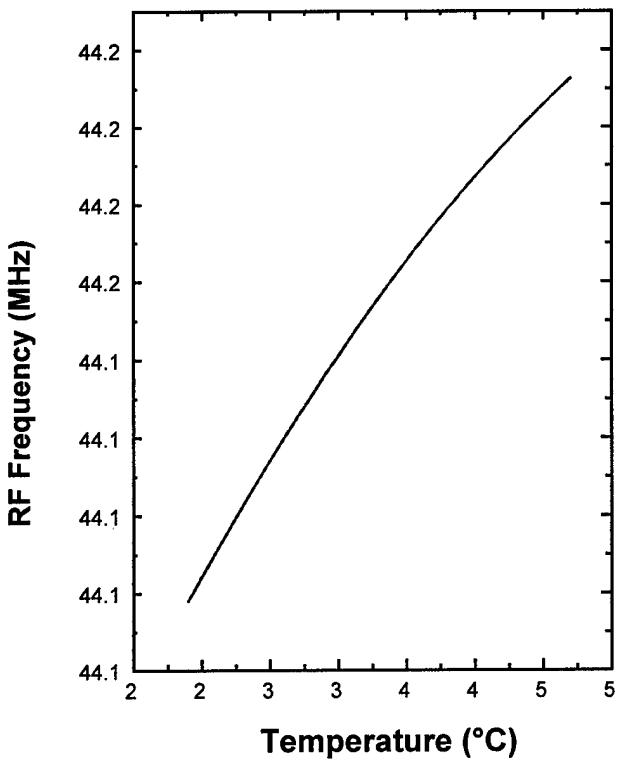

Figure 44 Measured Frequency as a function of Temperature

Since the AOTF bandwidth is less than the channel spacing, the cross state operation was chosen for the construction and test of the DFAE demo. The test was performed using three lasers at λ_1 = 1555nm, λ_2 = 1550nm and λ_3 = 1533nm, respectively. Figure 45 shows the measured output power spectra before and after the equalization. The maximum differential dynamic range between two signals is about 40dB.

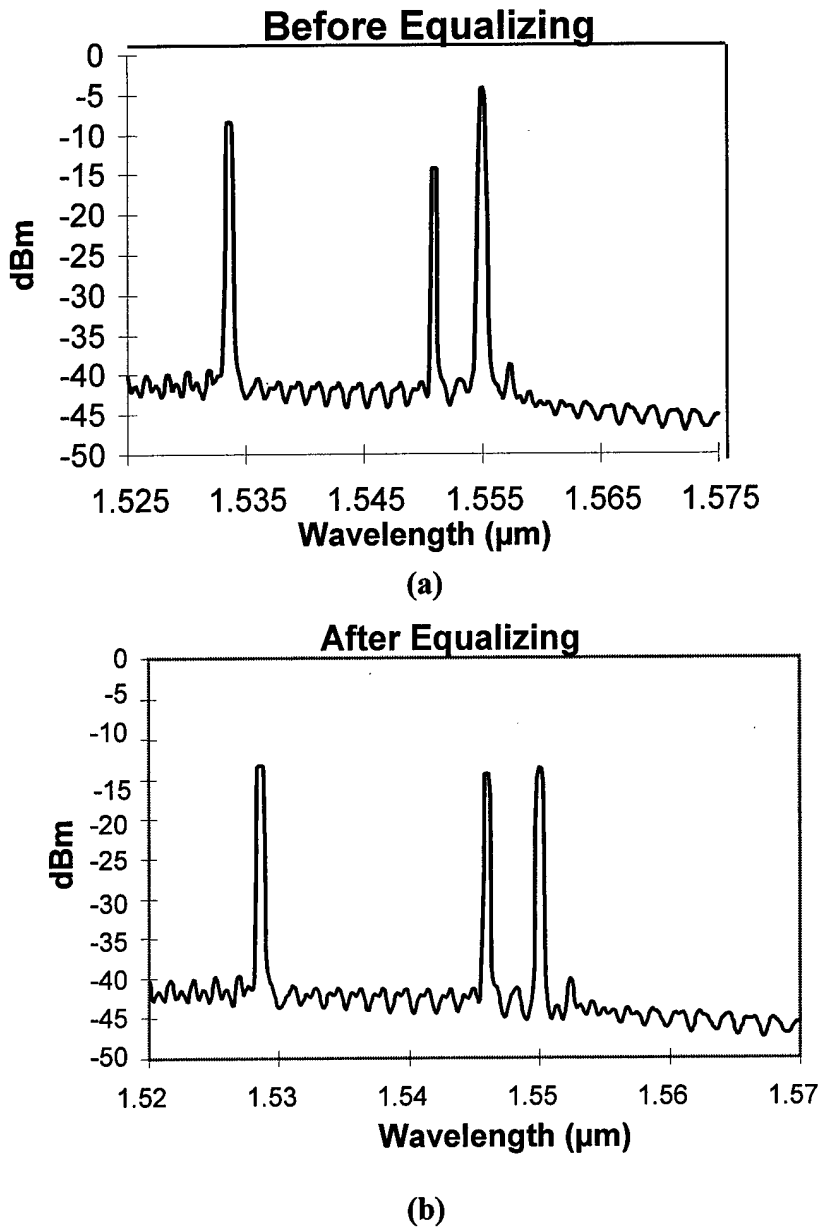

Figure 45 Measured WDM Spectral Output (a) Before and (b) After the Equalizer:

6.0 Conclusion

The deployment of passive dense (D) WDM into a point-to-point telecommunication network has realized the optical transport of wideband signals. The emerging WDM technology is now aimed at adding the functionality of switching, routing and management of the multi-wavelength signals in the optical domain. To achieve these goals, the key components needed are the dynamically reconfigurable optical add & drop multiplexer (OADM), optical cross-connect (OXC) and dynamic fiber amplifier equalizers (DFAE). The present approach is to use passive WDM to separate the multi-wave optical signals into many single wavelength channels and complete the desired operation using wavelength independent optical crossbars or multiport matrix switches. The optical hardware based on such SDM approach becomes increasingly

complex and costly as the number of wavelengths increases. An alternative approach is to realize the desired function in the multi-wavelength domain based on a multi-wave tunable filter. Compared to the space domain switches, the use of tunable filters or wavelength domain switches is more efficient for reconfigurable WDM networks at increasing number of wavelengths. The tunable filter approach is particularly economical for the optical interconnection with a small number of input and output ports.

The objective of this program is to implement the wavelength domain switch using a special bulkwave device known as the collinear beam (CB) AOTF. We have studied the basic characteristics and limitations of the CB AOTF. A variety of designs is developed for improving the device performance. Some of the proposed designs have been chosen in the experimental research of this project. Based on the theoretical and experimental findings, we have experimentally demonstrated filter bandpass response with low sidelobes at 100GHz channel spacing. The key performance parameters of the PI CBAOTF include: a FWHM of 0.5nm, sidelobe less than -25dB, optical insertion loss of 3dB, polarization dependent loss less than 0.1dB, and polarization mode dispersion of less than 1psec.

The use of the CBAOTF for dynamically reconfigurable components of OADM, OXC and DFAE are also investigated. The most critical limitation, crosstalk, is studied. A variety of architectures were proposed and examined for reducing crosstalk. Using a 2x2 AOTF as the wavelength-selective cross-connect (WSXC), crosstalk reduction architectures such as the space dilation structure are experimentally studied. The experimental work verifies the theoretical projections.

In another important application that shows a potential near-term commercial product, the CBAOTF were used as a feedback controlled multi-wave attenuator (MWA) to equalize the gain of fiber amplifiers. An 8-channel direct digital synthesizer (DDS) driver was constructed that provides 8 RF signals with programmable frequencies and power levels. The DDS driver is used to drive the AOTF-based MWA. A second PIAOTF was used as a WDM spectral monitor to provide the necessary information for feedback control.

Based on these theoretical and experimental results, the use of AOTF for implementation of the dynamic WDM components appears to be the most practical, low-cost approach compared to any of the presently available technologies. The realizable channel spacing is limited to 0.8nm or 100GHz. For even narrower channel spacings, wavelength dilation should be used, considering the overall system cost.

Although the minimum channel spacing sets a limit of the maximum number of channels, it is possible to increase the channel capacity by exploiting the extremely wide tuning range of the AOTF. Considering the progress of the EDFA, Raman amplifiers, and semiconductor optical filters (SOAs), it is expected that the usable wavelength range for future WDM systems could be extended to multiple bands covering the entire 1200 to 1700nm spectral range. The advanced AOTF technology developed under this program is expected to play a major role in these future optical transport and switching networks.

References

[1] C. A. Brackett et al "A Scalable Multiwavelength Multihop Optical Network: A Proposal for Research on All-Optical Networks," J. Lightwave Tech. 11, p. 736 (1993).

[2] K. McCammon et al, "Deployment of the National Transparent Optical Network around the San Francisco Bay Area," *National Fiber Optic Conference* (September 1996).

[3] D. A. Smith et al, "Evaluation of the Acousto-Optic Wavelength Routing Switch," J. Lightwave Tech. 14, p. 1005 (1996).

[4] S. E. Harris and R. W. Wallace "Acousto-Optic Tunable Filter," J. Opt. Soc. Am. 59, p. 744 (1969).

[5] I. C. Chang, "Acousto-Optic Tunable Filters," Opt. Eng. 20, p. 824 (1981).

[6] I. C. Chang, "Collinear Beam Acousto-Optic Tunable Filters," Elect. Lett. 28, p. 1255, (1992); Also, U.S. Patent No. 5,329,397.

[7] H. Hermann et al, "Polarization Independent, Integrated Optical, Acoustically Tunable Wavelength Filters/Switches with Tapered Acoustic Directional Coupler," Photon. Tech. Lett. 6, p. 1335 (1994).

[8] I. C. Chang, "Acousto-Optic Tunable Filters in Wavelength Division Multiplexing (WDM) Networks," *1997 Conference on Laser and Electro-Optics (CLEO)*, Baltimore, MD (May, 1997).

[9] I. C. Chang, "Progress of Acousto-Optic Tunable Filters," Proc. 1996 IEEE Ultrasonics Symposium, p. 819 (1996).

[10] I. C. Chang et al, "Bandpass Response of Collinear Beam Acousto-Optic Tunable Filters," IEEE Ultrasonics Symposium Proceedings, (Oct. 1997).

[11] I.C. Chang, "Acousto-Optic Switch for DWDM Network" Photonics Taiwan '98, Taipei, Taiwan (May, 1998).